Distribution Agreement

In presenting this thesis or dissertation as a partial fulfillment of the requirements for an advanced degree from Emory University, I hereby grant to Emory University and its agents the non-exclusive license to archive, make accessible, and display my thesis or dissertation in whole or in part in all forms of media, now or hereafter known, including display on the world wide web. I understand that I may select some access restrictions as part of the online submission of this thesis or dissertation. I retain all ownership rights to the copyright of the thesis or dissertation. I also retain the right to use in future works (such as articles or books) all or part of this thesis or dissertation.

Signature:

_____   _____

Hasan Palta   Date

Some Mathematical Problems in Design of Free-Form Mirrors and Lenses

By

Hasan Palta
Doctor of Philosophy

Mathematics

Vladimir I. Oliker, Ph.D.
Advisor

David Borthwick, Ph.D.
Committee Member

James Nagy, Ph.D.
Committee Member

Accepted:

Lisa A. Tedesco, Ph.D.
Dean of the James T. Laney School of Graduate Studies

Date

Some Mathematical Problems in Design of Free-Form Mirrors and Lenses

By

Hasan Palta
M.Sc., Emory University, 2010

Advisor: Vladimir I. Oliker, Ph.D.

An abstract of
A dissertation submitted to the Faculty of the
James T. Laney School of Graduate Studies of Emory University
in partial fulfillment of the requirements of the degree of
Doctor of Philosophy
in Mathematics
2012

Abstract

Some Mathematical Problems in Design of Free-Form Mirrors and Lenses
By Hasan Palta

In this dissertation, we investigate several optics-related problems. The problems discussed in Chapters 1, 2 and 3 are concerned with the determination of surfaces reshaping collimated beams of light to obtain a priori given intensities on prescribed target sets. In optics, such transformations are performed by lenses and/or mirrors whose shapes need to be determined in order to satisfy the application requirements. These are inverse problems, which in analytical formulations lead to nonlinear partial differential equations of Monge-Ampère type. In Chapter 4, we present several different designs of radiant energy concentrators. Our goal in these designs is to obtain a device that can capture solar rays with maximal efficiency.

Some Mathematical Problems in Design of Free-Form Mirrors and Lenses

By

Hasan Palta
M.Sc., Emory University, 2010

Advisor: Vladimir I. Oliker, Ph.D.

A dissertation submitted to the Faculty of the
James T. Laney School of Graduate Studies of Emory University
in partial fulfillment of the requirements of the degree of
Doctor of Philosophy
in Mathematics
2012

Acknowledgments

To my beloved wife and children...

Contents

List of Figures

List of Tables

List of Algorithms

Chapter 1

The Design of a Free-Form Lens

1.1 Introduction to the Problem

The lens design problem consists in determining a pair of refractive surfaces transforming an input plane wave of light with a given intensity distribution into a coherent plane wave of the same direction illuminating a given target set with a prescribed in advance output intensity. Many important practical applications of solutions to this problem and its extensions are possible. These include design of corrective lenses in ophthalmology (contact lenses and eyeglasses), imaging systems such as monoculars, binoculars, telescopes, microscopes, cameras and projectors, dielectric lenses, used in radio astronomy and radar systems and commonly called lens antennas, which are required to refract electromagnetic radiation into a collector antenna. The use of relatively large lenses to concentrate solar energy on small photovoltaic cells, harvesting more energy without the need to use larger and more expensive cells, is another important application.

Lens design problems have been extensively studied by many scientists in the past century. However, most of these studies treat this problem under the apriori assumption of rotational or some other symmetry of the data and solution. This assumption limits severely the flexibility of design

and excludes important applications in which such symmetries are not available. Consequently, in recent years there has been a huge surge in research in the field of design of free-form lenses and mirrors with the focus on the development of methods capable of designing lenses and mirrors without any apriori assumptions of symmetry of the data and solution. The two-lens problem discussed in this chapter is one of the central problems in this area.

Even in the rotationally symmetric case this problem is not simple and has been studied by many researchers. Pioneering work on this case was carried out by Frieden [5] and Kreuzer [13]. More recently, a special case leading to nonconvex free-form lenses was studied by Rubistein and Wolansky [24, 25]. These researchers developed a "weighted least action" principle based on a dynamic interpretation of the problem. In [20, 21] Oliker developed a geometric approach and, by combining it with methods of mass transport theory, he succeeded in building a comprehensive variational theory of weak solutions in all practically important cases.

In this chapter, we investigate an alternative approach in which the mass transport theory component in Oliker's work is replaced by a minimization method discovered earlier also by Oliker and applied by him and his research collaborators to various antenna and mirror design problems (see [1], [11], [12]). It was also used widely in the optics community (see [2], [3], [4], [14], [15], [17]). We show that this approach can also be used to investigate existence and uniqueness of solutions. Furthermore, this approach is constructive and we use it to develop a computational method for solving the problem numerically. The results of this chapter related to the existence of solutions in Section 1.5.2 and the method of constructing their numerical approximation in Section 1.6 are obtained jointly with Prof. V. Oliker.

We describe the problem as follows. Let us consider the Cartesian coor-

dinate system in $\mathbb{R}^{N+1}$ and let $(x, z) = (x_1, \ldots, x_N, z)$, where z is the vertical axis perpendicular to the hyperplane $\alpha := \{z = 0\}$. Let B_1 be a beam of light rays propagating parallel to the z-axis in the positive direction $\vec{k}$. Let us denote the intersection of the light beam with the plane α by $\bar{D}$, which is the closure of the bounded domain $D \subset \mathbb{R}^N$. These rays refract at two different surfaces in the following manner.
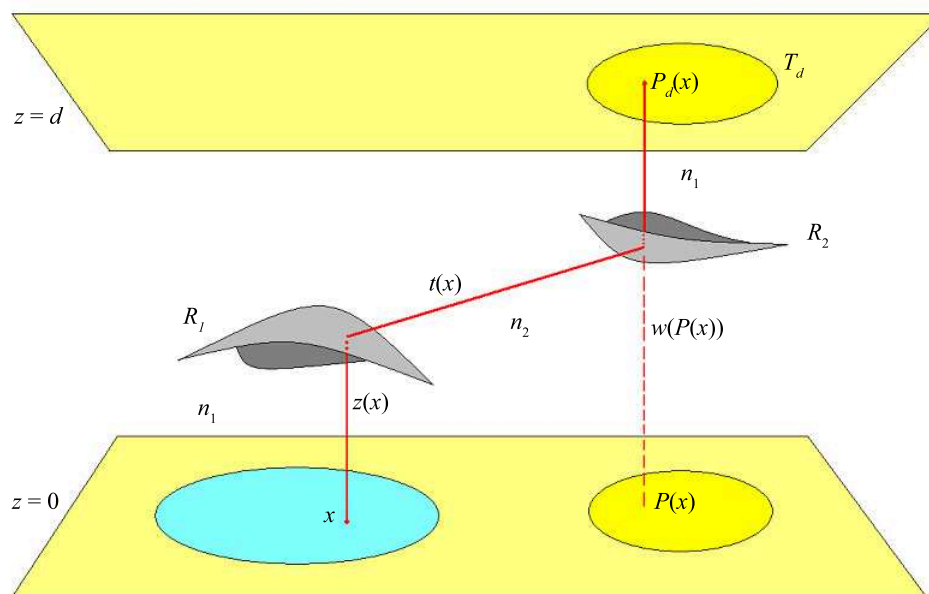
Figure 1.1: The lens design problem

Let $n > 0$ be the relative refractive index between two different media. That is, if medium I and medium II have refractive indices of $n_1 > 0$ and $n_2 > 0$, then $n = n_1/n_2$ (see Figure 1.1). This normalization permits us to think of medium I as having refractive index of n and medium II as having refractive index of 1. Define the first refractive surface R_1 by $(x, z(x)), x \in D$, where z is a smooth function. The rays in medium I refract at the surface R_1 and reach a second surface R_2. Then, they refract once again so as to

propagate parallel to the $\vec{k}$ direction again until they reach the hyperplane α_d, located at a distance $d > 0$ above the hyperplane α. The intersection of the light beam and the hyperplane α_d is denoted by $\bar{T}_d$, and the projection of the latter onto α by T. Note that the refractive index in the medium between R_2 and α_d is also equal to n. We can therefore label all the rays in the last medium as $(p, w(p)), p \in \bar{T}$, where w is a function defined on $\bar{T}$.

It is possible to track each ray by tracing the ray at $x \in \bar{D}$ reaching the point $(p, d) \in \bar{T}_d$. This would define a mapping $P_d : \bar{D} \rightarrow \bar{T}_d$, which can be rewritten as $P_d(x) = P(x) + d\vec{k}$.

Definition 1.1. *The mapping $P : \bar{D} \rightarrow \bar{T}$ is called the* refractor map.

The following physical quantities will be crucial in our work.

The *optical path length* (OPL) is defined by

$$l(x) := n \cdot z(x) + |(x, z(x)) - (P(x), w(P(x)))| + n \cdot (d - w(P(x))) \tag{1.1}$$

where the absolute value stands for the length of the vector. It is a fact that the OPL, $l(x) = l$, is constant. Also, the *input light intensity $I(x), x \in \bar{D}$*, will be the intensity of light entering the system through the hyperplane α. The *output light intensity $L(p), p \in \bar{T}$*, will be the intensity of the light reaching the hyperplane $\alpha_d = \{z = d\}$. We assume that the system is perfectly energy-preserving; i.e. no light (or energy) is lost during refraction. Therefore, the following equality holds:

$$\int_D I(x)dx = \int_T L(p)dp. \tag{1.2}$$

We consider a *two-lens system* where R_1 is the outer boundary to the top of a lens with the bottom side planar and perpendicular to the z-axis (which is actually inactive) and R_2 is the outer boundary to the bottom of another lens with the upper side of the lens planar and perpendicular to the z-axis (and thus inactive as well). Actually, without loss of generality, we can

consider the first lens as the region between α and R_1 and the second lens as the region between R_2 and α_d. Now, we can state the *two-lens problem*.

Let $d, l > 0$ and $n > 1$ be constants so that $l - nd \neq 0$. Let the compact regions $\bar{D} \subset \alpha$ and $\bar{T}_d \subset \alpha_d$ also be given and accompanied by the input intensity $I \in L^1(\bar{D})$, $I \geq 0$, $I \not\equiv 0$ and supp$(I) \in \bar{D}$. Let the output intensity be given by a Radon measure μ defined on $\bar{T}$. We are required to find the two surfaces R_1 and R_2 such that:

1. The beam of light penetrating into the system at the hyperplane α travels through medium I with index of refraction n in direction $\vec{k}$ and refracts at the surface R_1 and then moves through medium II with refractive index 1 until it reaches the second refracting surface R_2, where the rays will refract once again and enter the last medium with refractive index n again and continue their trajectories also in direction $\vec{k}$ until they finally reach the target set $\bar{T}_d$.

2. The input intensity $I(x)$ on $\bar{D}$ is transformed by the mapping P_d into the intensity distribution μ on $\bar{T}_d$. (Write $\mu(U)$ for any Borel set $U \in \bar{T}$).

3. The OPL is set as a constant:

$$l(x) = l, \forall x \in \bar{D}$$

4. In order to make physical sense, the surfaces R_1 and R_2 are required not to intersect; that is,

$$z(x) < w(p), \forall (x, p) \in \bar{D} \times \bar{T}$$

1.2   The PDE Describing the Two-Lens Problem

We apply two fundamental principles of geometrical optics to derive the differential equation:

1. Snell's Law of Refraction

2. The conservation of energy law for energy transfer along infinitesimally small tubes of rays throughout the system.

The constancy of the OPL is a corollary of Snell's Law of Refraction and the requirement that the input and output fronts are parallel and both orthogonal to the z-axis [20].

Snell's Law also implies that the refracted ray at R_1 has the direction

$$\vec{y} = n \cdot \vec{k} + \frac{M - n}{\sqrt{1 + |\nabla z|^2}} \vec{n} \tag{1.3}$$

where $\vec{n}$ is the unit normal vector field on R_1 and

$$M = \sqrt{1 + (1 - n^2)|\nabla z|^2}. \tag{1.4}$$

A necessary physical condition is that $\langle \vec{n}, \vec{k} \rangle > 0$. Introduce the *reduced optical path length* (ROPL) $\beta = l - nd$. Note here that the ROPL could be either positive or negative depending on the way the problem is constructed.

The domains $\bar{D}$ and $\bar{T}$ are connected via the mapping

$$P(x) = x - \frac{\beta}{M} \nabla z, x \in \bar{D}. \tag{1.5}$$

In order for P to make physical sense, we need to have $1 + (1 - n^2)|\nabla z|^2 > 0$ or

$$|\nabla z|^2 < \frac{1}{n^2 - 1}.$$

Recall that the lenses are considered to be energy-preserving. So, the input energy

$$\int_W I(x) dx \tag{1.6}$$

is redirected and redistributed over $P_d(W)$ for any subset $W \subset D$. The expansion (or contraction ratio) is given by $\frac{1}{J(P_d)}$ where J is the Jacobian

operator. As a result, the Radon measure $\mu = L(p)dp$ on $\bar{T}$ for $L \in L^1(\bar{T}), L \geq 0$, together with the input density $I(x)dx$ are connected via the PDE

$$L(P(x)) |J(P(x))| = I(x), \forall x \in \bar{D}. \tag{1.7}$$

In summary, the two-lens design problem for smooth solutions is as follows:

Suppose we are given bounded open domains $D, T \subset \alpha = \{z = 0\}$ with smooth boundaries, non-negative functions $I \in L^1(\bar{D}), L \in L^1(\bar{T})$ and numbers $n > 1, l$ and $d > 0$ such that

$$\beta = l - nd \neq 0. \tag{1.8}$$

The class of smooth solutions to the lens problem requires:

1. The determination of $z \in C^2(D) \cap C^1(\bar{D})$ such that $P : \bar{D} \rightarrow \bar{T}$ is surjective (onto).

2. The relation $I(x) = |J(P(x))| \cdot L(P(x))$ be satisfied in D.

The graph of a function z describes the surface R_1. The second refracting surface R_2 is given by the function:

$$w(P(x)) = z(x) + \frac{\beta}{1 - n^2}\left(n + \frac{1}{M}\right), x \in \bar{D}, \tag{1.9}$$

where $M = \sqrt{1 + (1 - n^2)|\nabla z|^2}$. The requirement that $w(p) > z(x), \forall (x, p) \in \bar{D} \times \bar{T}$ implies the condition $\frac{\beta}{1-n^2} > 0$ or $\beta < 0 \Leftrightarrow n > 1$.

1.3   Geometry of Refractors

1.3.1   Refracting Hyperboloids

Let $n > 1$ and $\beta < 0$ be given constants. For a quadruple $(x, p, \xi, \eta) \in \alpha^2 \times \mathbb{R}^2$, put

$$\hat{l}(x) = \sqrt{|x - p|^2 + (\xi - \eta)^2} - n \cdot (\eta - \xi).$$

Now, set $c(x,p) = \sqrt{\beta^2 + (n^2 - 1)\left|x - p\right|^2}$. Note that since $\beta < 0$ and $n > 1$, this quantity is well-defined. Also define

$$C(x,p) = \frac{n\beta - c(x,p)}{n^2 - 1}. \tag{1.10}$$

Lemma 1.2. *If $n > 1$, then for any arbitrary fixed $(p, \eta) \in \alpha \times \mathbb{R}$, the equation*

$$\hat{l}(x, p, \xi, \eta) = \beta \tag{1.11}$$

uniquely defines the function

$$\xi^l_{p,\eta}(x) = C(x,p) + \eta, x \in \alpha, \tag{1.12}$$

whose graph is the lower branch of a two-sheeted hyperboloid of revolution about the z-axis with foci at

$$F^l_{p,\eta} = \left(p, \eta + \frac{2n\beta}{n^2 - 1}\right) \text{ and } F^u_{p,\eta} = (p, \eta).$$

The center of the hyperboloid is located at $\left(p, \eta + \frac{n\beta}{n^2-1}\right)$, and the eccentricity is equal to n.

  Similarly, for any arbitrary fixed $(x, \xi) \in \alpha \times \mathbb{R}$, the equation $\hat{l}(x, p, \xi, \eta) = \beta$ uniquely defines the function

$$\eta^u_{x,\xi}(p) = -C(x,p) + \xi, p \in \alpha, \tag{1.13}$$

whose graph is the upper branch of a two-sheeted hyperboloid of revolution about the z-axis with foci at

$$F^l_{x,\xi} = (x, \xi) \text{ and } F^u_{x,\xi} = \left(x, \xi - \frac{2n\beta}{n^2 - 1}\right).$$

The center of the hyperboloid is located at $\left(x, \xi - \frac{n\beta}{n^2-1}\right)$, and the eccentricity is equal to n.

Proof. First, by multiplying the expression $\hat{l}(x, p, \xi, \eta) - \beta = 0$ with the conjugate $\sqrt{|x-p|^2 + (\xi - \eta)^2} + n \cdot (\eta - \xi) + \beta$ and using some simple algebra techniques, we obtain the following

$$\frac{\left\{\xi - \left(\eta + \frac{n\beta}{n^2-1}\right)\right\}^2}{\frac{\beta^2}{(n^2-1)^2}} - \frac{(x-p)^2}{\frac{\beta^2}{n^2-1}} = 1. \tag{1.14}$$

This is a quadric of revolution with the semi-axes $\frac{|\beta|}{|n^2-1|}$ and $\frac{|\beta|}{\sqrt{n^2-1}}$. Now, for fixed (x, ξ) and (p, η), we can solve for $y := \eta - \xi$ and get the following pair of solutions:

$$y_1(x,p) = \frac{-n\beta + c(x,p)}{n^2 - 1} \text{ and } y_2(x,p) = \frac{-n\beta - c(x,p)}{n^2 - 1} \tag{1.15}$$

Since $n > 1$, we see that y_1 solves the equation $\hat{l}(x, p, \xi, \eta) - \beta = 0$. The other statements follow immediately from elementary properties of conics. □

Lemma 1.3. *Let $n > 1$ and $(p, \eta) \in \alpha \times \mathbb{R}$ be fixed. Then, for each $x \in \alpha$, the ray in direction $\vec{k}$ through x below the graph of $\xi^l_{p,\eta}$ will refract at $\left(x, \xi^l_{p,\eta}(x)\right)$ with refraction index $n > 1$ and $\beta < 0$. All such rays will pass through the focus $F^u_{p,\eta} = (p, \eta)$.*

Proof. By Lemma 1.2, we have that the upper focus is $F^u_{p,\eta} = (p, \eta)$. A ray originating at the point $(x, \xi^l_{p,\eta}(x))$ and passing through $F^u_{p,\eta}$ can be given by

$$\vec{y'}(x) = \frac{\left(p - x, \eta - \xi^l_{p,\eta}(x)\right)}{\sqrt{|p - x|^2 + (\eta - \xi^l_{p,\eta}(x))^2}}. \tag{1.16}$$

We need to show that $\vec{y'}(x) = \vec{y}(x)$ where $\vec{y}(x)$ is given in (1.3) with $z = \xi^l_{p,\eta}$. Let the projections of y and y' on the surface $z = 0$ be y_0 and y'_0, respectively. Using Lemma 1.2, we have

$$\sqrt{|p - x|^2 + (\eta - \xi^l_{p,\eta}(x))^2} = \beta - n\left(\xi^l_{p,\eta}(x) - \eta\right) = \beta - nC(x,p) = \frac{n \cdot (x,p) - \beta}{n^2 - 1}. \tag{1.17}$$

Here, $n > 1$ and $\beta < 0$ implies that $n \cdot (x, p) - \beta \geq n|\beta| - \beta = -\beta(n + 1) > 0$ for all x and p. Then,

$$y_0' = \frac{p - x}{\sqrt{|p - x|^2 + (\eta - \xi_{p,\eta}^l(x))^2}} = \frac{(n^2 - 1)(p - x)}{n \cdot c(x, p) - \beta}. \tag{1.18}$$

On the other hand, by the definition of $\xi_{p,\eta}^l$,

$$\nabla_x \xi_{p,\eta}^l = -\frac{\nabla c(x, p)}{n^2 - 1} = -\frac{x - p}{c(x, p)} \tag{1.19}$$

where ∇_x is the gradient operator with respect to the variable x. By the definition (1.4) of M, we also have that $M = \frac{|\beta|}{c(x,p)}$. The unit normal field on the graph of $z = \xi_{p,\eta}$ is

$$\vec{n}(x) = \frac{\left(\nabla \xi_{p,\eta}^l(x), 1\right)}{\sqrt{1 + \left|\nabla \xi_{p,\eta}^l(x)\right|^2}} \tag{1.20}$$

Therefore,

$$y_0 = -\frac{M(x) - n}{1 + \left|\nabla \xi_{p,\eta}(x)\right|^2} \nabla \xi_{p,\eta}(x) = -\frac{\beta + n \cdot c(x, p)}{\beta^2 + n^2 \left|x - p\right|^2}(x - p) \tag{1.21}$$

It follows that $y_0' = y_0$ from the fact that

$$(\beta - n \cdot c(x, p))(\beta + n \cdot c(x, p)) = -(n^2 - 1)(\beta^2 + n^2(x - p)^2).$$

The equality $y_z' = y_z$ where the subscript describes the projection onto the z-axis can be shown similarly. $\qquad \square$

Remark 1.4. *An analogous restatement of Lemma 1.3 can be derived for the other branch of the hyperboloid of revolution given by (1.13).*

Lemma 1.5. *Suppose $n > 1$ and $\beta < 0$. If $(\bar{p}, \bar{\eta}) \in \alpha \times \mathbb{R}$ is fixed and $\xi_{\bar{p},\bar{\eta}}^l$ is the lower branch of a hyperboloid of revolution defined as in the previous lemma.*

Then, for each $x \in \alpha$, the graph of the branch $\eta^u_{x,\xi^l_{\bar{p},\bar{\eta}}(x)}(p), p \in \alpha$ passes through $(\bar{p}, \bar{\eta})$. The ray originated from $\left(x, \xi^l_{\bar{p},\bar{\eta}}\right)$ and passing through $(\bar{p}, \bar{\eta})$ is refracted by the branch $\eta^r_{x,\xi^l_{\bar{p},\bar{\eta}}(x)}$ with refraction index n and direction $\vec{k}$.

Proof. First, pick a point $\bar{x} \in \alpha$. It follows from Lemma 1.2 that $\bar{\xi} := \xi^l_{\bar{p},\bar{\eta}}(\bar{x}) = C(\bar{x}, \bar{p}) + \bar{\eta}$ and $\eta^u_{\bar{x},\bar{\xi}}(\bar{p}) = -C(\bar{x}, \bar{p}) + \bar{\xi}$. Then, $\eta^r_{\bar{x},\bar{\xi}}(\bar{p}) = \bar{\eta}$.

Now, the ray can be tracked as follows. Let $\vec{V}$ be the directed ray from $(\bar{x}, \bar{\xi})$ to $(\bar{p}, \bar{\eta})$. Consider the vertical ray in the negative vertical direction propagating down from $+\infty$ and hitting the sheet $\eta^u_{\bar{x},\bar{\xi}}$ at the point $(\bar{p}, \bar{\eta}) = (\bar{p}, \eta^u_{\bar{x},\bar{\xi}}(\bar{p}))$. By Lemma 1.3, the refracted ray will pass through the point $(\bar{x}, \bar{\xi})$ which is equivalent to the directed ray $-\vec{V}$. This proves the claim. □

1.4 General Refracting Surfaces

The lemmas above can be summarized in the following theorem:

Theorem 1.6. *Let R_1 and R_2 be the two refracting surfaces of a lens system with refraction index $n > 1$, separation $d > 0$ and reduced optical path length $\beta = l - nd < 0$. Let R_1 and R_2 be the graphs of the functions $z \in C^1(\bar{D})$ and $w \in C^1(\bar{T})$, respectively. Assume that the mapping $P : \bar{D} \to \bar{T}$ is a diffeomorphism. Fix some point $(\bar{x}, z(\bar{x})) \in R_1$ and let $(\bar{p} = P(\bar{x}), w(\bar{p})) \in R_2$.*

Then $z(\bar{x}) = \xi^l_{\bar{p},\bar{\eta}}(\bar{x})$, where $\xi^l_{\bar{p},\bar{\eta}}$ is the lower branch of the hyperboloid of revolution defined by

$$\xi^l_{\bar{p},\bar{\eta}}(x) = C(x, \bar{p}) + \bar{\eta}, x \in \alpha \tag{1.22}$$

with upper focus at $F^u_{\bar{p}} = (\bar{p}, w(\bar{p}))$. In addition, the tangent hyperplanes to R_1 at $(\bar{x}, z(\bar{x}))$ and to the graph of $\xi^l_{\bar{p},\bar{\eta}}(x)$ at $\bar{x}$ coincide.

Similarly, $w(\bar{p}) = \eta^u_{\bar{x},z(\bar{x})}(\bar{p})$ where $\eta^u_{\bar{x},z(\bar{x})}$ is the upper branch of the two-sheeted surface of revolution defined by

$$\eta^u_{\bar{x},z(\bar{x})}(p) = -C(\bar{x}, p) + z(\bar{x}), p \in \alpha \tag{1.23}$$

and $F_{\bar{x}}^l = (\bar{x}, z(\bar{x}))$ is the lower focus. In addition, the tangent hyperplanes to R_2 at $(\bar{p}, w(\bar{p}))$ and to the graph of $\eta_{\bar{x},z(\bar{x})}^u(x)$ at $\bar{p}$ coincide.

Moreover, the tangent hyperplanes to R_1 at $(\bar{x}, z(\bar{x}))$ and to R_2 at $(\bar{p}, w(\bar{p}))$ are parallel.

Proof. Let $x \in D$ and set $p = P(x)$. Then the functions $z(x)$ and $w(p) = w(P(x))$ satisfy the relation (1.11) as

$$\hat{l}(x, p, z, w) = \beta. \tag{1.24}$$

Let $\bar{x}$ and $\bar{p} = P(\bar{x})$ be defined as in the hypothesis. Put $p = \hat{p}$ and $w = w(\hat{p})$ in (1.24). Since the mapping P is a diffeomorphism from D to T, by Lemma 1.2, we have that the graph of the lower branch is given by $z(\bar{x}) = \xi_{\bar{p},w(\bar{p})}^l(\bar{x})$ whose upper focus is located at $F_{\hat{p}}^u = (\bar{p}, w(\bar{p}))$. We can combine (1.5) and the equality (1.19) derived in the proof of Lemma 1.3 and get:

$$\bar{p} - \bar{x} = \nabla \xi_{\bar{p},w(\bar{p})}^l(\bar{x}) c(\bar{x}, \bar{p}) = -\frac{\beta}{M} \nabla z(\bar{x}). \tag{1.25}$$

In other words, since $\beta < 0$, the gradients of $\xi_{\bar{p},w(\bar{p})}^l$ and z have the same direction at the point $\bar{x}$. Therefore, the normal vectors to the surface R_1 and the graph of $\xi_{\bar{p},w(\bar{p})}^l$ at $(\bar{x}, z(\bar{x}))$ coincide. So, for each point $(x, z(x)) \in R_1$ and its corresponding point $(p, w(p)) \in R_2$ where $p = P(x)$, there is only one hyperboloid of revolution whose lower branch is tangent to the surface R_1 at the point $(x, z(x))$ and having the upper focus at $(p, w(p)) \in R_2$.

More generally, the surface R_1 is an envelope of the family of lower sheets of hyperboloids of revolution whose upper foci are located on the surface R_2. Reverting the statements for R_1 and R_2, we can also say that the surface R_2 is an envelope of the family of upper sheets of hyperboloids of revolution whose lower foci are located on the surface R_1. By similar arguments as above, the surface R_2 and the graph of $\eta_{x,z(x)}^u$ have a common normal vector at the point $(p, w(p))$ when $x = P^{-1}(p)$. Indeed, using the

definition of $\eta^u_{x,z(x)}$ in (1.23), we have

$$x - p = \nabla \eta^u_{x,z(x)}(p)c(x,p). \qquad (1.26)$$

Now, considering the expressions (1.25) and (1.26) together, we can conclude that the tangent hyperplanes to R_1 at $(x, z(x))$ and to R_2 at $(p, w(p))$ will be parallel, provided that $p = P(x)$. This completes the proof of the theorem. □

The formal definition of a lens is given below.

Definition 1.7. *Let $n > 1$ and $\beta < 0$. A pair $(z, w) \in C(\bar{D}) \times C(\bar{T})$ is called a* lens *if*

$$z(x) = \inf_{p \in \bar{T}} \{C(x, p) + w(p)\}, \forall x \in \bar{D} \qquad (1.27)$$

and

$$w(p) = \sup_{x \in \bar{D}} \{-C(x, p) + z(x)\}, \forall p \in \bar{T}. \qquad (1.28)$$

In a lens, the refractor map *and its inverse, the* visibility map, *are defined by:*

$$P_{z,w}(x) = \{p \in \bar{T} : z(x) = C(x, p) + w(p)\}, x \in \bar{D} \qquad (1.29)$$

and

$$P^{-1}_{z,w}(p) = \{x \in \bar{D} : w(p) = -C(x, p) + z(x)\}, p \in \bar{T}. \qquad (1.30)$$

1.5 The Existence of a Solution

1.5.1 Preliminaries

Although the construction of the problem is valid for any finite dimension N, it would be convenient to consider the 3-dimensional case where the refractor surfaces are given by graphs over domains in the 2-dimensional plane $\alpha = \{(x, y, z) \in \mathbb{R}^2 : z = 0\}$. From now on, we assume that light is

emitted through a domain $D = \{x \in \mathbb{R}^2 : I(x) > 0\}$ where $I : \mathbb{R}^2 \to \mathbb{R}^+$ is the input density function. Let $T \subset \mathbb{R}^2$ be a compact set, which is the target domain of the problem. Let

$$\xi_{p,\eta}(x) = \frac{n\beta - \sqrt{\beta^2 + (n^2 - 1)\left|x - p\right|^2}}{n^2 - 1} + \eta \tag{1.31}$$

be the graph of the lower branch of a two-sheeted hyperboloid of revolution about the z-axis with foci at

$$F_{p,\eta}^l = \left(p, \eta + \frac{2n\beta}{n^2 - 1}\right) \text{ and } F_{p,\eta}^u = (p, \eta). \tag{1.32}$$

The solid convex body bounded by $\xi_{p,\eta}(x)$ is denoted by $B_{p,\eta}(x)$ and let

$$B_{p,\eta} = \bigcap_{x \in D} B_{p,\eta}(x) \text{ and } \mathcal{R}_{p,\eta} = \partial B_{p,\eta}.$$

Assume that for any $p \in T$, we have η so large that $B_{p,\eta} \supset D \cup T$.

Definition 1.8. $\mathcal{R}_{p,\eta}$ *or shortly* $\mathcal{R}$, *is called a (convex) refractor constructed from the family of hyperboloids* $\xi_{p,\eta}(x)$.

Let $\mathcal{R}$ be a (convex) refractor and $\xi_{p,\eta}(x)$ be a hyperboloid of revolution bounding the body B that contains D.

Definition 1.9. *If* $\xi_{p,\eta}(x) \cap \mathcal{R} \neq \varnothing$, *that is,* $\exists q \in \xi_{p,\eta}(x) \cap \mathcal{R}$, *then we say that* $\xi_{p,\eta}(x)$ *is a supporting hyperboloid to* $\mathcal{R}$ *at* q.

In our constructions, the domains D and T remain fixed. From the last definition, it follows that for every $r \in \mathcal{R}$, there is at least one hyperboloid of revolution from the family $\{\xi_{p,\eta}(x), p \in T\}$.

Definition 1.10. *If there exist more than one supporting hyperboloid at some point* $r \in \mathcal{R}$, *the point* r *is singular* .

Note that any tangent plane to a supporting hyperboloid at a point of contact with $\mathcal{R}$ is also a supporting plane to $\mathcal{R}$. Therefore, any singular point on $\mathcal{R}$ is also singular in the sense of convexity theory. In other words, at such a point there is more than one supporting hyperplane to $\mathcal{R}$. Recall also that by Reidemeister's theorem, the set of singular points on $\mathcal{R}$ has measure 0 (zero).

Let $U \subset T$ be a subset and define the set

$$M(U) = \left\{ q \in \mathcal{R} : \exists x \in U \text{ such that } \xi_{p,\eta}(x) \text{ is supporting to } \mathcal{R} \text{ at } z \right\}. \quad (1.33)$$

By convexity of $\mathcal{R}$ and the assumption that $\xi_{p,\eta}(x) > 0$ for all $x \in D$, we can consider the orthogonal projection of $\mathcal{R}$ onto α along vertical rays through D.

Definition 1.11. *The image set of $M(U)$ under orthogonal projection on D is called the visibility set of U and is identical to $P_{z,w}^{-1}(U)$ where $P_{z,w}^{-1} : T \to D$ is the inverse of the refractor map. The visibility set of U will be denoted by $V(U)$.*

In other words, the visibility set $V(U) = P_{z,w}^{-1}(U)$ is the set of all points $x \in D \subset \mathbb{R}^2$ being a preimage of a point in the target domain T.

The following chain of lemmas will be used to show that if $U \subset T$ is a Borel set, then $V(U)$ is a measurable set on D.

Lemma 1.12. *If $U \subset \bar{T}$ is closed, then $V(U)$ is also closed.*

Proof. Assume that U is a closed subset of T. Let $\{x_i\}_{i=1}^{\infty}$ be a sequence converging to some point $\bar{x}$ in D. Also, let $p_i \in P_{z,w}(x_i)$ and select a converging subsequence $\{p_{i_k}\}$ of $\{p_i\}$. Now, let $H_{p_{i_k}}$ be the corresponding hyperboloid of revolution which is supporting to the refractor $\mathcal{R}$ at the point $z(x_{i_k})$. Note that each $H_{p_{i_k}}$ is determined by p_{i_k} and $z(x_{i_k})$. Then, the sequence $\left\{ H_{p_{i_k}} \right\}$ will converge to some hyperboloid $H_{\bar{p}}$ and we will have $z(\bar{x}) \in H_{\bar{p}}$. In the meantime, since each hyperboloid $H_{p_{i_k}}$ is supporting to $\mathcal{R}$, so is $H_{\bar{p}}$. Therefore, $z(\bar{x}) \in M(U)$ and $\bar{x} \in V(U)$. As a result, $V(U)$ is closed. $\qquad \square$

Lemma 1.13. *Let $U_1, U_2 \subset \bar{T}$ and $U_1 \cap U_2 = \varnothing$. Then $\mu\left(V(U_1) \cap V(U_2)\right) = 0$ where μ is the standard Lebesgue measure on α.*

Proof. Assume that $x \in V(U_1) \cap V(U_2)$. Then there are at least two hyperboloids of revolution that are supporting to the refractor $\mathcal{R}$ at the point $z(x)$. Therefore, $z(x)$ is a singular point of the refractor. By Reidemeister's theorem, the set of singular point of a set has zero volume. So, the lemma follows. □

Lemma 1.14. *Let $U_i \subset \bar{T}; i = 1, 2, \ldots$ and $U = \bigcup_{i=1}^{\infty} U_i$. Then, $V(U) = \bigcup_{i=1}^{\infty} V(U_i)$. Also, if each $V(U_i)$ is measurable, so is $V(U)$.*

Proof. Suppose that $x \in V(U)$. Then there exists a supporting hyperboloid of revolution at $(x, z(x))$ with focus at $(p, w(p))$ where $p \in U$. So, $p = P_{z,w}(x) \in U_i$ for some i. Then, $x \in V(U_i)$ fore some i. Therefore, $x \in \bigcup_{i=1}^{\infty} U_i$. The converse is obvious. □

Lemma 1.15. *If $U \subset \bar{T}$ and $V(U)$ is measurable, then so is $V(\bar{T} \backslash U)$.*

Proof. Consider the disjoint union

$$V\left(\bar{T} \backslash U\right) = \left(V(\bar{T}) \backslash V(U)\right) \cup \left(V(\bar{T} \backslash U) \cap V(U)\right).$$

Here, by Lemma 1.13, we have $\mu\left(V(\bar{T} \backslash U) \cap V(U)\right) = 0$. Also, by assumption, $V(U)$ is measurable and since $V(\bar{T})$ is closed and measurable, then $V(\bar{T} \backslash U)$ is also measurable. □

Lemma 1.16. *Let $U = \bigcap_{i=1}^{\infty} U_i$ and suppose $V(U_i)$ is measurable for each i. Then $V(U)$ is also measurable.*

Proof. We can rewrite this intersection as

$$U = \bar{T} \backslash \bigcup_{i=1}^{\infty} (\bar{T} \backslash U_i).$$

By Lemma 1.15, $V(\bar{T} \backslash U)$ is measurable and by Lemma 1.14, $\bigcup_{i=1}^{\infty} (\bar{T} \backslash U_i)$ is measurable. Therefore, $\bigcap_{i=1}^{\infty} U_i$ is measurable. □

Lemma 1.17. *If $U \subset \bar{T}$ is an open subset, then $V(U)$ is a measurable subset of $\bar{D}$.*

Proof. Clearly, we have that $\bar{T} \backslash U$ is closed. Set $\omega := \mu\left(V(\bar{T} \backslash U) \cap V(U)\right)$. Now, since $(\bar{T} \backslash U) \cap U = \varnothing$, it follows from Lemma 1.13 that $\mu(\omega) = 0$. Note also that we can write the domain D as the following disjoint union of its subsets:

$$D = \omega \bigcup \left(V(\bar{T} \backslash U) \backslash \omega\right) \bigcup \left(V(U) \backslash \omega\right).$$

Here, the sets D, ω, $V(\bar{T} \backslash U) \backslash \omega$ are all measurable sets. Then, $V(U) \backslash \omega$ is measurable, and thus, $V(U)$ is measurable. $\qquad\square$

Lemma 1.18. *If $U_i \subset \bar{T}$ for each $i = 1, 2, \ldots$, and $\cap_{i=1}^{\infty} U_i = \varnothing$ then $\lim_{i \to \infty} \mu(V(U_i)) = 0$.*

Proof. We here have two cases:

1. If $\cap_{i=1}^{\infty} V(U_i) = \varnothing$, then obviously, we have $\lim_{i \to \infty} \mu(V(U_i)) = 0$.

2. If $\cap_{i=1}^{\infty} V(U_i) \neq \varnothing$, choose some point $x \in \cap_{i=1}^{\infty} V(U_i)$. Then $P_{z,w}(x) \in U_i$ for all $i = 1, 2, \ldots$. Then $z(x)$ is a singular point and then $\mu\left(\cap_{i=1}^{\infty} V(U_i)\right) = 0$, so finally, $\lim_{i \to \infty} \mu(V(U_i)) = 0$.

$\qquad\square$

Theorem 1.19. *If $U \subset T$ is a Borel set, then the visibility set $V(U)$ is measurable.*

Proof. The proof is a result of the Lemmas 1.12-1.18 $\qquad\square$

1.5.2 The Existence Theorem

Let the intensity on the closed simply connected set D be a non-negative continuous function $I(x)$ and let $I \equiv 0$ outside the set D. Consider a Borel subset $U \in \mathcal{B}(T)$ of $\bar{T}$, a two-lens represented by the pair (z, w), a refractor

map $P = P_{z,w} : D \rightarrow T$ and the set $V(U) = P_{z,w}^{-1}(U)$, which is Lebesgue measurable due to Teorem 1.5.1. Define the following measure:

$$G_{z,w}(U) = \int_{V(U)} I(x)dx. \tag{1.34}$$

Here, $G_{z,w}$ may not be absolutely continuous but it can be shown to be a non-negative additive and finite measure on the σ-algebra of $\mathcal{B}(\bar{T})$. The function $G_{z,w}(U)$, describes the total amount of energy that is transferred from the set $V(U)$ to $U \subset T$ via the refractor $\mathcal{R}$.

On the other hand, for any Borel set $U \subset \bar{T}$, define a measure on T with $L : \bar{T} \rightarrow \mathbb{R}^+, L \in L^1(\bar{T})$ by

$$F(U) = \int_U L(p)dp. \tag{1.35}$$

where dp will be the measure on the set T.

Definition 1.20. *We say that a (convex) refractor $\mathcal{R}$ is a weak solution of the refractor problem if*

$$G_{z,w}(U) = F(U) \tag{1.36}$$

for any Borel set $U \subset \bar{T}$.

Before stating the existence theorem, we introduce another couple of lemmas:

Lemma 1.21. *Let $\mathcal{R}^k$, $k = 1, 2, \ldots$ be a sequence of refractors given by the pairs (z_k, w_k) with a common initial domain D converging to a refractor $\mathcal{R}$. Assume also that $P_{z_k,w_k}(D) = T$ for each k. Then, for any point $z(x) \in \mathcal{R}$, there is a hyperboloid of revolution $H(x)$ supporting to the refractor $\mathcal{R}$ at $z(x)$ with focus at $(p = P(x), w(p))$.*

Proof. Let $r \in \mathcal{R}$ be fixed and choose a sequence of points $\{r_k\}_{k=1}^{\infty} \subset \mathcal{R}$ such that $r_k \rightarrow r$ as $k \rightarrow \infty$. Let $H^k(p_k)$ be a hyperboloid of revolution that is

supporting to $\mathcal{R}^k$ at r_k. Then, there is a subsequence $\{H_{k_j}\}$ of hyperboloids that converge to H and is supporting to $\mathcal{R}$ at r. In addition, we have that $p_k \in T$ for each k and the subsequence $\{p_{k_j}\}$ converges to $p \in T$. Then, the required supporting hyperboloid is constructed and the lemma is proved.

$\square$

Lemma 1.22. *With the same hypothesis of Lemma 1.21, the sequence of measures G_{z_k,w_k} corresponding to the refractors $\mathcal{R}^k$ converges weakly to the measure $G_{z,w}$ corresponding to the refractor $\mathcal{R}$.*

Proof. By Lemmas 1.12-1.18 and 1.21, we can define the measure $G_{z,w}$ on T by

$$G_{z,w}(U) = \int_{V(U)} I(x)d\mu_x. \tag{1.37}$$

Let $p = P(x)$ and $p_k = P(x_k)$ be the points on T corresponding to the foci points of the hyperboloids of revolution $H(p)$ and $H^k(p_k)$ that are supporting to the refractors $\mathcal{R}$ and $\mathcal{R}^k$, respectively. Then, if f is a continuous function on T, we can write

$$\int_T f\,dG_{z_k,w_k} = \int_D f(p_k(x))I(x)d\mu_x \text{ and } \int_T f\,dG_{z,w} = \int_D f(p(x))I(x)d\mu_x. \tag{1.38}$$

Now, consider the sets U and U_k of points in D such that the images $P_{z,w}(x)$ and $P_{z_k,w_k}(x_k)$ are multi-valued, i.e. contains more than one point. Then, the corresponding points r, r_k of the refractors $\mathcal{R}$ and $\mathcal{R}^k$ are singular points, and by Reidemeister's theorem, $\mu(U) = \mu(U_k) = 0$. Setting $\bar{U} = U \cup \bigcup_{k=1}^{\infty} U_k$, then, we also have $\mu(\bar{U}) = 0$. Therefore, the integrals in (1.38) are defined almost everywhere. Now, given any point $x \in \bar{U}$, the sequence $\{H^k(p_k)\}$ of hyperboloids converges to the hyperboloid $H(p)$. So we have $p_k(x) \to p(x)$, and then $f(p_k(x)) \to f(p(x))$ almost everywhere. Consequently, since the point x and the function f are arbitrary, we deduce

$$\int_T f\,dG_{z_k,w_k} \to \int_T f\,dG_{z,w}. \tag{1.39}$$

□

The following existence theorem, obtained jointly with Prof. V. Oliker, is the main result of this chapter:

Theorem 1.23. *Let T be a compact subset in $\mathbb{R}^2$. Let $I \in L^1(\bar{D})$ and $L \in L^1(\bar{T})$ with $I, L \geq 0$. Assuming that the total energy condition (1.2) holds, there is a (convex) refractor $\mathcal{R}$ satisfying (1.36) for any Borel set $U \subset \bar{T}$.*

Proof. To prove the theorem, we first consider the measure F as being concentrated at a finite number of points, i.e. we can write $T = \{p_1, p_2, \ldots, p_N\}$. So F would be a sum of Dirac measures F^k. In this case, the refractor problem can be solved using a finite number of hyperboloids of revolution with foci at the points $p_k, k = 1, \ldots, N$. Next, we use the weak continuity of the measures to establish a weak solution to the refractor problem satisfying (1.36) by letting $N \to \infty$.

Let $\varepsilon > 0$. Given any integer $N \in \mathbb{N}^+$, we divide the set T into disjoint Borel sets $U_1^N, \ldots, U_N^N$ in the following manner. For any $\varepsilon > 0$, there is a number K such that if $N > K$, we have $\text{diam}(U_i^N) < \varepsilon$ for each $i = 1, \ldots, N$. Now, from each set U_i^N, pick any point p_i^N. We set the following measure

$$F_i^N = \int_{U_i^N} L(p) d\mu_p. \tag{1.40}$$

So, if $U \in \mathcal{B}(T)$ is a Borel set in T, the following finite measure can be defined

$$F^N(U) = \sum_{p_i^N \in U_i^N} F_i^N. \tag{1.41}$$

If we let $N \to \infty$, then the measure F^N will converge weakly to the measure F defined in (1.35). On the other hand, by Theorem 1.26 (proved below), there exists a refractor $\mathcal{R}^N$ such that for each $i = 1, \ldots, N$, we have

$$G(p_i^N)) = F_i^N. \tag{1.42}$$

Defining the measure G^N for any Borel set $U \in \mathcal{B}(T)$ by

$$G^N(U) = \sum_{p_i^N \in U_i^N} G(p_i^N)), \tag{1.43}$$

we see that the equality $G^N = F^N$ holds for any $N \in \mathbb{N}$.

For each $N \in \mathbb{N}$, by Theorem 1.29 proved in Section 1.7 and by fixing only one of the supporting hyperboloids, the set of all hyperboloids that are supporting to $\mathcal{R}^N$ is bounded on D. Then, the sequence of refractors $\{\mathcal{R}^N\}$ must be bounded. By the Blaschke selection theorem, there is a subsequence $\{\mathcal{R}^{N_k}\}$ of $\{\mathcal{R}^N\}$ which is convergent to a convex surface $\mathcal{R}$. This completes the proof. □

1.5.3 Refractors Defined by a Finite Number of Hyperboloids

Assume that

$$M = \sup_{x \in D, p \in T} |x - p| \tag{1.44}$$

Also, denote by $\mathcal{H}$ the set of all hyperboloids of revolution $H(\eta)$ with axes of symmetry passing through (p, η). In order to make physical sense, the parameter η needs to be large enough so that the whole hyperboloid of revolution lies above both sets D and T.

Let $K \geq 2$ be an integer and the set T be a discrete set. So we can write

$$T = \{p_1, \ldots, p_K\}. \tag{1.45}$$

Let η_i be K real numbers and H_i be hyperboloids of revolution from the set $\mathcal{H}$.

As in Section 1.5.1, denote by B_i the convex body bounded by the hyperboloid H_i and put

$$B = \bigcap_{i=1}^{K} B_i. \tag{1.46}$$

As a result of the fact that each η is large, we have for each $i = 1, \ldots, K$ that $T \subset B_i$ and thus $T \subset B$.

From now on, given a set of points $\{p_1, \ldots, p_K\}$, the surface $R = \partial B$ will be convex (since each branch of hyperboloid is convex). As the refractor R can be totally determined by those numbers, it will be convenient to denote it by the K-tuple $(\eta_1, \ldots, \eta_K)$. Then the visibility sets $V(p_i)$ corresponding to each point p_i together with the corresponding measures $G_i := G(p_i)$ can be defined accordingly as in Section 1.5.2. We will use the notation $G = (G_1, \ldots, G_K)$ to denote the vector of intensities on the entire refractor $\mathcal{R}$ corresponding to the points $p_1, \ldots, p_K$. In particular, a hyperboloid of revolution H_{i_0} in the family $\mathcal{H}$ that is not supporting to the refractor $\mathcal{R}$ will collect no energy sent through the initial domain D. In this case, we will have simply $G_{i_0} = 0$.

We now need the following result:

Lemma 1.24. *Consider the two refractors* $\left(\eta_1, \ldots, \eta_j, \ldots, \eta_K\right)$ *and* $\left(\eta_1, \ldots, \bar{\eta}_j, \ldots, \eta_K\right)$ *with respective measure function G and $\bar{G}$. In this case,*

$$\eta_j \leq \bar{\eta}_j \Rightarrow G_j \geq \bar{G}_j \text{ and } G_i \leq \bar{G}_i \text{ if } i \neq j. \tag{1.47}$$

Proof. Let $V(p_k)$ be the visibility set of the first refractor given by

$$V(p_k) = \left\{ x \in D : \frac{n\beta - c(x, p_k)}{n^2 - 1} + \eta_k \leq \frac{n\beta - c(x, p_j)}{n^2 - 1} + \eta_j, k \neq j \right\} \tag{1.48}$$

where $c(x, p) = \sqrt{\beta^2 + (n^2 - 1)\left|x - p\right|^2}$ as in Section 1.3. Here, by setting $k = j$, we have that if $\bar{\eta}_j \leq \eta_j$ then $V(p_j) \subset \bar{V}(p_j)$ where $\bar{V}$ is the visibility set of the second refractor. This implies that $G_j \leq \bar{G}_j$. For all other indices $i \neq j$, similarly, we have again by (1.48) that $V(p_i) \supset \bar{V}(p_i)$ and then $G_i \geq \bar{G}_i$, which completes the proof. □

The following is a result of Lemma 1.24

Lemma 1.25. *Let* $(\bar{\eta}_1, \ldots, \bar{\eta}_K)$ *and* $(\hat{\eta}_1, \ldots, \hat{\eta}_K)$ *represent two refractors with respective measures* $\bar{G}$ *and* $\hat{G}$. *Set a new refractor by* $\eta_i = \min(\bar{\eta}_i, \hat{\eta}_i)$ *and define its measure to be G. Then, for each* $i = 1, \ldots, K$, *we will have*

$$G_i \leq \max\left(\bar{G}_i, \hat{G}_i\right). \tag{1.49}$$

Proof. It is easy to see here that only two cases are possible. Either we have $\eta_i = \bar{\eta}_i$, which implies $G_i \leq \bar{G}_i$ or $\eta_i = \hat{\eta}_i$, which implies $G_i \leq \hat{G}_i$. The result follows. $\qquad\square$

The existence theorem for the refractor constructed by a finite number of hyperboloids can be given as follows.

Theorem 1.26. *Assume that* $I \in L^1(D)$ *is a non-negative integrable function. Let* $T = \{p_1, \ldots, p_K\}$ *where* $K \geq 2$. *Also, let* $f_1, \ldots, f_K$ *be non-negative numbers satisfying*

$$\int_D I(x)dx = \sum_{i=1}^{K} f_i. \tag{1.50}$$

Then, there is a refractor R constructed using a finite number of hyperboloids of revolution $H_1 = H(p_1), \ldots, H_K = H(p_K)$ *for some corresponding* $\eta_1, \ldots, \eta_K$. *The corresponding visibility sets* $V_1, \ldots, V_K$ *will be covering the initial domain D in such a way that for each* $i = 1, \ldots, K$,

$$\mu(V_\alpha \cap V_\beta) = 0 \text{ for any } \alpha \neq \beta \text{ and } P_{z,w}(V_i) = p_i. \tag{1.51}$$

$$G_i = f_i. \tag{1.52}$$

Proof. Assume that $f_j \neq 0$ for some $1 \leq j \leq K$ (Otherwise, the integral is zero and there is nothing to prove). Set $\eta_j = h$ for some level h in such a way that $G_i = G(p_i) \leq f_i$ for all $i \neq j$. This means that all hyperboloids H^i with indices $i \neq j$ are collecting at most the amount of energy prescribed for each target point $p_i \in T$. Let us denote the set of all such refractors by $\mathcal{REF}$.

Clearly, it is easy to see that the set $\mathcal{REF}$ is non-empty. To prove it, we can simply construct a refractor $\mathcal{R}_0$ by setting $\eta_j = h$ and setting $\eta_i = h + S$ for all parameters with indices $i \neq j$ where $h > 0$ and $S = \frac{2L}{\sqrt{n^2-1}}$ (see Section 1.7). In this case, none of the hyperboloids of revolution H^i will be collecting any energy, except for H^j which will be the only supporting hyperboloid of the refractor $\mathcal{R}_0$. Therefore, we will have

$$G_j = \int_D I(x) d\mu_x \text{ and } G_i = 0, \forall i \neq j. \tag{1.53}$$

Then, $\mathcal{R}_0 \in \mathcal{REF}$. Note also that the family of all visibility sets $V_1, \ldots, V_K$ defined in (1.51) forms a cover of the initial domain D.

Next, define a refractor $\bar{\mathcal{R}} \in \mathcal{REF}$ by setting

$$\bar{\eta}_j = \eta_j \text{ and } \bar{\eta}_i = \inf_{\mathcal{R} \in \mathcal{REF}} \eta_i, \forall i \neq j. \tag{1.54}$$

Our claim is that $\bar{\mathcal{R}}$ is solving the refractor problem and satisfies the conditions (1.51) and (1.52). Let us now verify these properties.

By Lemma 1.22, the following holds: If the refractors $(\eta_1^\varepsilon, \ldots, \eta_K^\varepsilon) \rightarrow (\eta_1, \ldots, \eta_K)$ as $\varepsilon \rightarrow 0$, then for the corresponding measures, we have $G_i^\varepsilon \rightarrow G_i$ for each $i = 1, \ldots, K$. Since the refractor $\bar{\mathcal{R}}$ is in the set $\mathcal{REF}$, it is true that

$$G_i \leq f_i. \tag{1.55}$$

We are claiming that the equality holds. Assume conversely that fome some index i_0, the strict inequality $G_{i_0} < f_{i_0}$ holds. In this case, by the continuity of the measures, there would be some $\varepsilon > 0$ such that $G_{i_0} < G_{i_0}^\varepsilon < f_{i_0}$. Here $G_{i_0}^\varepsilon$ is the measure corresponding to the refractor with parameters $(\bar{\eta}_1, \ldots, \bar{\eta}_{i_0} - \varepsilon, \ldots, \bar{\eta}_K)$. Here we have $G_i^\varepsilon \leq f_i$ for each $i \neq i_0$ and $i \neq j$. Therefore, by Lemma (1.25), we have here that $G_j^\varepsilon \geq f_j > 0$. Then, the hyperboloids of revolution H^j and H^{i_0} are both supporting to the refractor $\bar{\mathcal{R}}^\varepsilon$. Therefore, $\bar{\mathcal{R}}^\varepsilon \in \mathcal{REF}$. This contradicts the way the refractor $\bar{\mathcal{R}}$ was constructed. As a result the equality $G_i = f_i$ must be true for each $i \neq j$.

Since the sum of the measures must add up to the total energy through the domain D, we must also have $G_j = f_j$. So the refractor $(\bar{\eta}_1, \ldots, \bar{\eta}_K)$ satisfies the condition (1.52). □

1.5.4 A Uniqueness Theorem

Note that the refractor satisfying the condition (1.52) is unique in the sense described in the following theorem.

Theorem 1.27. *Let the density function $I(x) > 0$ almost everywhere on D and suppose that there are two refractors $(\bar{\eta}_1, \ldots, \bar{\eta}_K)$ and $(\hat{\eta}_1, \ldots, \hat{\eta}_K)$ satisfying (1.52). Then,*

$$\text{if } \bar{\eta}_j \leq \hat{\eta}_j \text{ for some } j \Rightarrow \bar{\eta}_i \leq \hat{\eta}_i, \forall i = 1, \ldots, K. \tag{1.56}$$

In particular,

$$\text{if } \bar{\eta}_j = \hat{\eta}_j \text{ for some } j \Rightarrow \bar{\eta}_i = \hat{\eta}_i, \forall i = 1, \ldots, K. \tag{1.57}$$

Proof. Let both of the refractors $(\bar{\eta}_1, \ldots, \bar{\eta}_K)$ and $(\hat{\eta}_1, \ldots, \hat{\eta}_K)$ satisfy (1.52). Consider the set of indices $J = \{j | \bar{\mu} > \hat{\mu}, 1 \leq j \leq K\}$.

Assume that $J \neq \varnothing$. Define a set $\{p_j | j \in J\}$. Choose a point x from the visibility set $\bar{V} = \bar{V}\left(\{p_j | j \in J\}\right)$. Then there is an index $j_0 \in J$ such that

$$C(x, p_{j_0}) + \bar{\eta}_{j_0} \leq C(x, p_i) + \bar{\eta}_i \text{ for any } i \notin J. \tag{1.58}$$

In addition, we have

$$C(x, p_j) + \hat{\eta}_j < C(x, p_j) + \bar{\eta}_j, \text{ for any } j \in J \tag{1.59}$$

and

$$C(x, p_i) + \hat{\eta}_i \geq C(x, p_i) + \bar{\eta}_i, \text{ for any } i \notin J. \tag{1.60}$$

Combining (1.58), (1.59) and (1.60), we obtain

$$C(x, p_{j_0}) + \hat{\eta}_{j_0} < C(x, p_i) + \bar{\eta}_i \text{ for any } i \notin J. \tag{1.61}$$

As a result, for the corresponding intensities, we get the following strict inequality

$$f_i = \bar{G}_i(p_i) < \hat{G}_i(p_i) = f_i. \tag{1.62}$$

This contradiction implies that J must be empty. So the result (1.56) follows.

The result in (1.57) can be shown by combining the statement in (1.56) together with the same argument with the inequalities reversed. $\quad\square$

1.6 The Method of Supporting Hyperboloids and the Algorithm

In this section, we describe the method of supporting hyperboloids and present an algorithm that can be implemented using any programming tool to solve the discrete version of the refractor problem. This is a joint work with Prof. V. Oliker.

Consider the same domain D with density function $I \in L^1(\bar{D})$ as before. Let the set T consist of a finite set of points $p_1, \ldots, p_K$ and let the density L on T be replaced by the discrete measure

$$F_K = \sum_{k=1}^{K} f_k \cdot \delta(p_k) \tag{1.63}$$

concentrated at the points $p_1, \ldots, p_K$. The discrete version of the problem requires us to construct a refractor $\mathcal{R}_K$ that refracts light to the points $p_1, \ldots, p_K$ in such a way that the total energy sent to each point p_k is equal to f_k.

It is natural to construct this refractor $\mathcal{R}_K$ by hyperboloids of revolution with axes passing through the points $p_1, \ldots, p_K$ and parameters $\eta_1, \ldots, \eta_K$ such that

$$z_{p_k,\eta_k}(x) = \frac{n\beta - \sqrt{\beta^2 + (n^2 - 1)\left|x - p_k\right|^2}}{n^2 - 1} + \eta_k := C(x, p_k) + \eta_k. \tag{1.64}$$

The graph of the function in (1.64) gives the lower branch of the required hyperboloid. The corresponding upper branch to refract the rays in positive direction $\vec{k}$ will be

$$w_{x,z_{p_k,\eta_k}(x)}(p_k) = -C(x,p_k) + z_{p_k,\eta_k}(x). \tag{1.65}$$

Definition 1.28. *The refractor $\mathcal{R}_K$ defined by a finite number of hyperboloids of revolution $H_1, \ldots, H_K$ is given by*

$$R_K = \partial\left(\bigcap_{k=1}^{K} B_k\right) \tag{1.66}$$

where B_k is the convex body bounded by H_k and ∂ stands for the boundary.

Note here that when the points $p_1, \ldots, p_K$ are fixed, we can completely identify the refractor $\mathcal{R}_K$ with the K-tuple $(\eta_1, \ldots, \eta_K)$. Define the measure $G_i(\mathcal{R}_K)$ for each point p_i by:

$$G_i(\mathcal{R}_K) = \int_{P_{z,w}^{-1}(p_i)} I(x)dx. \tag{1.67}$$

The discrete version of the problem would then be to find a refractor $\bar{\mathcal{R}}_K$ such that for each $i = 1, \ldots, K$, we have

$$G_i\left(\bar{\mathcal{R}}_K\right) = f_i. \tag{1.68}$$

The energy conservation law requires that

$$\mathcal{T} := \int_D I = \sum_{i=1}^{K} f_i. \tag{1.69}$$

Therefore, for any $\varepsilon > 0$, we can construct a solution refractor $\mathcal{R}_N$, where $N = N(\varepsilon)$ such that

$$\sum_{i=1}^{K} \left(G_i(\mathcal{R}_N) - f_i\right)^2 < \varepsilon^2. \tag{1.70}$$

We can now describe the algorithm. The aim is to find an approximate solution $\mathcal{R}_N$ to (1.68) such that $\|G - F\|_2 < \varepsilon$ where $G = (G_1, \ldots, G_K)$ and $F = (f_1, \ldots, f_K)$. Here, $\|\cdot\|_2$ is the usual Euclidean 2-norm. We now fix $\varepsilon > 0$, and one of the parameters, say $\eta_1 = \bar{\eta}$. Choose all other parameters $\eta_i, i = 2, \ldots, K$ large enough so that for those indices $i = 2, \ldots, K$, we have $G_i(\bar{\eta}, \eta_2, \ldots, \eta_K) \leq f_i$. Let us call $\mathcal{A}$ the set of all admissible refractors satisfying this condition. The implementation can be initialized with any refractor in $\mathcal{A}$. Then, the algorithm generates a sequence of refractors in $\mathcal{A}$ that is monotonically convergent to the solution of the problem. The algorithm is as follows:

Initialize:

1. the precision $\varepsilon > 0$,

2. the domain D and the target set $\{p_1, \ldots, p_K\}$,

3. the initial density $I : D \to \mathbb{R}^+$,

4. the prescribed densities $F = (f_1, \ldots, f_K)$,

5. the first guess refractor $Z = (\bar{\eta}, \eta_2, \ldots, \eta_K)$,

6. the initial step vector $S = (0, 1, \ldots, 1)$.

The main iteration is as follows:

Algorithm 1 The Method of Supporting Hyperboloids: The Algorithm

> **while** $\left\|G - f\right\|_2 \geq \varepsilon$ **do**
>> $\tilde{Z} \leftarrow Z - S.$
>> Update G for temporary vector $\tilde{Z}$.
>> **if** $\tilde{Z} \in \mathcal{A}$, i.e. $f_i > G_i, \forall i = 2, \ldots, K$ **then**
>>> $Z \leftarrow \tilde{Z}.$
>> **else** $\{\tilde{Z} \notin \mathcal{A}$, i.e. $\exists J \subset \{2, \ldots, K\}$ such that $f_j < G_j, \forall j \in J.\}$
>>> **while** $(Z - S) \notin \mathcal{A}$ **do**
>>>> **if** $j \in J$ **then**
>>>>> $S(j) \leftarrow S(j)/2.$
>>>> **end if**
>>> **end while**
>> **end if**
> **end while**

Evidently, for the initial guess refractor, we can choose the parameters $\eta_2, \ldots, \eta_K$ so large that the initial density is $G^{(0)} = (\mathcal{T}, 0, \ldots, 0)$, where $\mathcal{T} = \int_D I(x)dx$; that is, the first hyperboloid is closest to the plane α and captures all the light emitted through D.

1.7 An Estimate of the Parameters η_i

Theorem 1.29. *For any pair of indices $i \neq j$, we have the estimate*

$$\left|\eta_i - \eta_j\right| \leq \frac{L}{\sqrt{n^2 - 1}} \tag{1.71}$$

where

$$L = \max_{x \in D, p_i \in T} \left|x - p_i\right|. \tag{1.72}$$

Proof. Consider two different hyperboloids of revolution H^i and H^j defined on the same domain D and whose graphs are given by the equations $z_i(x) = C(x, p_i) + \eta_i$ and $z_j(x) = C(x, p_j) + \eta_j$, respectively. Here the function $C(x, p)$ is given by (1.10). For abbreviation, we can denote these hyperboloids in terms of their parameters η_i and η_j. We need to satisfy two conditions in order for both hyperboloids to be supporting to the refractor:

$$1. \quad \max_{x \in D} \left\{ C(x, p_j) + \eta_j \right\} \geq \min_{x \in D} \left\{ C(x, p_i) + \eta_i \right\} \tag{1.73}$$

$$2. \quad \min_{x \in D} \left\{ C(x, p_j) + \eta_j \right\} \leq \max_{x \in D} \left\{ C(x, p_i) + \eta_i \right\} \tag{1.74}$$

We set

$$\min_{x \in D, p \in T} |x - p| = 0 \text{ and } \max_{x \in D, p \in T} |x - p| = L. \tag{1.75}$$

Since the sets D and T are compact, the min and max are attained on $D \times T$. Doind some simple algebraic manipulations, and considering the fact that $\beta < 0$ and $n > 1$, from (1.73), we get

$$\eta_j - \eta_i \geq \frac{|\beta| - \sqrt{\beta^2 + (n^2 - 1)L^2}}{n^2 - 1} \tag{1.76}$$

and from (1.74), we get

$$\eta_j - \eta_i \leq \frac{-|\beta| + \sqrt{\beta^2 + (n^2 - 1)L^2}}{n^2 - 1}. \tag{1.77}$$

Combining the results in (1.76) and (1.77), we can write

$$\left| \eta_j - \eta_i \right| \leq \frac{-|\beta| + \sqrt{\beta^2 + (n^2 - 1)L^2}}{n^2 - 1}. \tag{1.78}$$

If $a, b > 0$, we have the inequality $\sqrt{a^2 + b^2} - a \leq b$. Then we can further simplify the estimate (1.78) and write

$$\left| \eta_j - \eta_i \right| \leq \frac{L}{\sqrt{n^2 - 1}}. \tag{1.79}$$

$\square$

1.8 Examples

In this section, we present several examples that were computed using the algorithm described in Section 1.6. We suppose that both $D = T = [-1, 1] \times [-1, 1]$. We initialize the parameter η_1 located at the center $(0, 0)$ as $\eta_1 = 3$.

In the first example, we take $K = 5$ points with $I \equiv 1$ and $\varepsilon = 0.01$. Our algorithm requires only 6 iterations to obtain the solution $(\eta_1, \eta_2, \eta_3, \eta_4, \eta_5)$. Table 1.1 below shows the values of the prescribed and obtained data. Recall that the vector $f = (f_1, \ldots, f_K)$ stands for the required distribution and $G = (G_1, \ldots, G_K)$ for the resulting distribution over the target points in T. The generated pair of surfaces representing the solution to the problem with 5 points is given in Figure 1.2.

Table 1.1: $K = 5$ points (Example 1)

i	p_i	η_i	f_i	G_i
1	(0,0)	3.0000	0.8080	0.8385
2	(-1,-1)	4.1015	0.8080	0.8004
3	(-1,1)	4.1015	0.8080	0.8004
4	(1,-1)	4.1015	0.8080	0.8004
5	(1,1)	4.1015	0.8080	0.8004

Apparently, when K is small, the result can be obtained very quickly. The following examples show how fast the number of iterations required to solve the problem increases as we discretize the target T by a larger number of points.

For Example 2, let $K = 17$. To compare with the first example, we take again $I \equiv 1$ and $\varepsilon = 0.01$. In this case, the solution is obtained in 60 iterations. Table 1.2 shows the resulting data. The surfaces of the lens
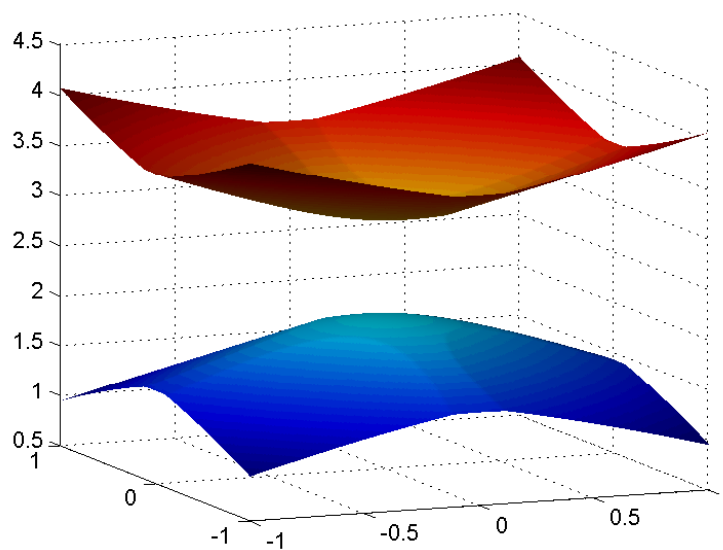
Figure 1.2: Lens design with 5 target points

solving this problem with 17 target points is given in Figure 1.3.

Table 1.2: $K = 17$ points (Example 2)

i	p_i	η_i	f_i	G_i
1	(0,0)	3.0000	0.2377	0.2777
2	(-1 , -1)	4.1138	0.2377	0.2373
3	(-1 , 1)	4.1138	0.2377	0.2373
4	(1 , -1)	4.1138	0.2377	0.2373
5	(1 , 1)	4.1138	0.2377	0.2373
6	(-1 , -1/3)	3.8049	0.2377	0.2297
7	(-1/3 , -1)	3.8049	0.2377	0.2297
8	(-1/3 , 1)	3.8049	0.2377	0.2297

Continued on next page

Table 1.2 – *Continued from previous page*

i	p_i	η_i	f_i	G_i
9	(1 , -1/3)	3.8049	0.2377	0.2297
10	(-1 , 1/3)	3.8049	0.2377	0.2360
11	(1/3 , -1)	3.8049	0.2377	0.2360
12	(1/3 , 1)	3.8049	0.2377	0.2360
13	(1 , 1/3)	3.8049	0.2377	0.2360
14	(-1/3 , -1/3)	3.3002	0.2377	0.2376
15	(-1/3 , 1/3)	3.3002	0.2377	0.2376
16	(1/3 ,-1/3)	3.3002	0.2377	0.2376
17	(1/3 , 1/3)	3.3002	0.2377	0.2376

Figure 1.3: Lens design with 17 target points

We finish this section by giving a last example using now $K = 37$ points for the target set T. Again we take $I \equiv 1$ and $\varepsilon = 0.01$. In this case, the algorithm needs 371 iterations 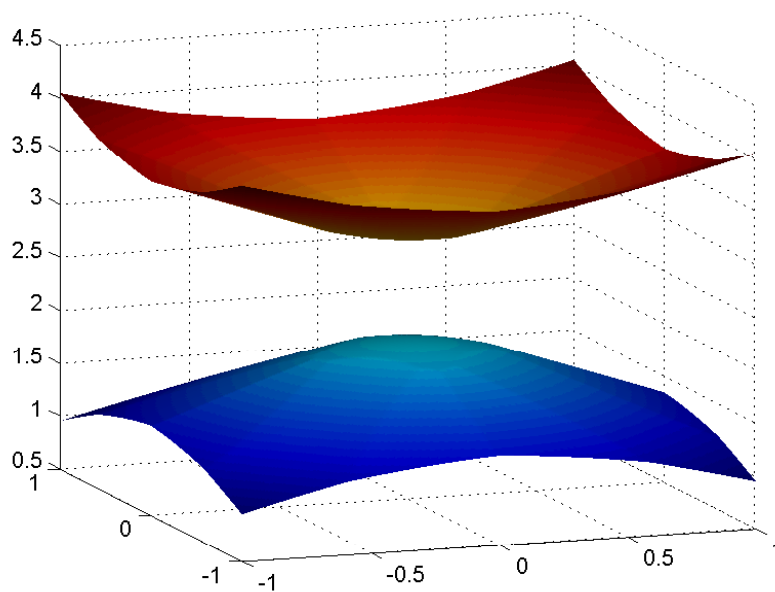to reach the solution. The resulting data obtained is presented in Table 1.3. The graph representing the corresponding lens is given in Figure 1.4.

Table 1.3: $K = 37$ points (Example 3)

i	p_i	η_i	f_i	G_i
1	(0 , 0)	3.0000	0.1086	0.1487
2	(-1 , -1)	4.1071	0.1086	0.1077
3	(-1 , 1)	4.1071	0.1086	0.1077
4	(1 , -1)	4.1071	0.1086	0.1077
5	(1 , 1)	4.1071	0.1086	0.1077
6	(-1 , -0.6)	3.8909	0.1086	0.1086
7	(-1 , 0.6)	3.8909	0.1086	0.1086
8	(-0.6 , -1)	3.8909	0.1086	0.1086
9	(-0.6 , 1)	3.8909	0.1086	0.1086
10	(0.6 , -1)	3.8909	0.1086	0.1086
11	(0.6 , 1)	3.8909	0.1086	0.1086
12	(1 , -0.6)	3.8909	0.1086	0.1086
13	(1 , 0.6)	3.8909	0.1086	0.1086
14	(-1 , 0.2)	3.7626	0.1086	0.1085
15	(0.2 , -1)	3.7626	0.1086	0.1085
16	(0.2 , 1)	3.7626	0.1086	0.1085
17	(1 , 0.2)	3.7626	0.1086	0.1085
18	(-1 , -0.2)	3.7626	0.1086	0.1058
19	(-0.2 , -1)	3.7626	0.1086	0.1058
20	(-0.2 , 1)	3.7626	0.1086	0.1058

Continued on next page

Table 1.3 – *Continued from previous page*

i	p_i	η_i	f_i	G_i
21	(1 , -0.2)	3.7626	0.1086	0.1058
22	(-0.6 , -0.6)	3.6126	0.1086	0.1080
23	(-0.6 , 0.6)	3.6126	0.1086	0.1080
24	(0.6 , -0.6)	3.6126	0.1086	0.1080
25	(0.6 , 0.6)	3.6126	0.1086	0.1080
26	(-0.6 , -0.2)	3.4300	0.1086	0.1057
27	(-0.2 , -0.6)	3.4300	0.1086	0.1057
28	(-0.2 , 0.6)	3.4300	0.1086	0.1057
29	(0.6 , -0.2)	3.4300	0.1086	0.1057
30	(-0.6 , 0.2)	3.4300	0.1086	0.1065
31	(0.2 , -0.6)	3.4300	0.1086	0.1065
32	(0.2 , 0.6)	3.4300	0.1086	0.1065
33	(0.6 , 0.2)	3.4300	0.1086	0.1065
34	(-0.2 , -0.2)	3.1456	0.1086	0.1085
35	(-0.2 , 0.2)	3.1456	0.1086	0.1085
36	(0.2 , -0.2)	3.1456	0.1086	0.1085
37	(0.2 , 0.2)	3.1456	0.1086	0.1085

1.9   Conclusion

In this chapter, we introduced the problem of designing a lens by approaching the solution numerically using geometric and optical properties of hyperboloids of revolution. The existence of a weak solution together with a numerical method of solving the problem is also presented. We also describe the uniqueness of the solution for the case of a finite number of hyperboloids. Oliker [21] proved existence and uniqueness of weak solu-
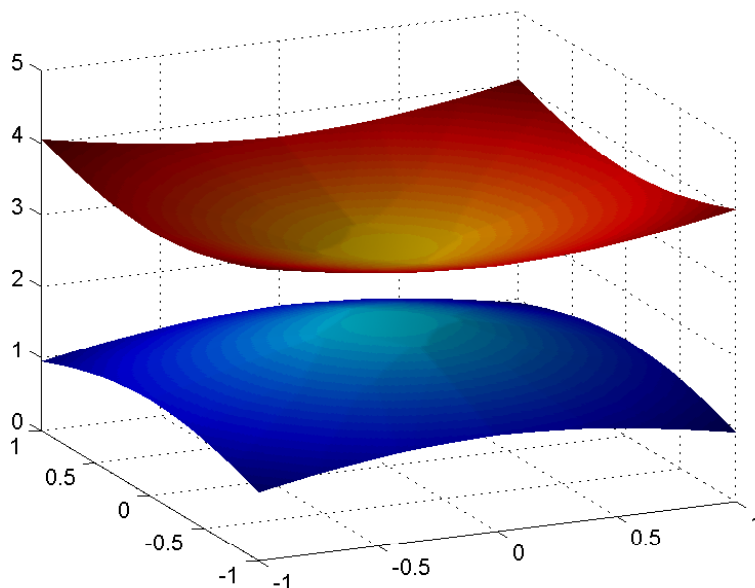
Figure 1.4: Lens design with 37 target points

tions in Lipschitz classes to problems requiring single- and two-refracting lenses. His method uses the framework of optimal mass transportation theory. The important concepts in Oliker's solution are those of a weak solution and refractor map.

The method of finitely many supporting hyperboloids is a method similar to that in [12]. It is based on formulating a finite-dimensional analogue of the problem for a special class of quadrics and solving first the corresponding discrete version.

As we see from our results, the algorithm associated to this method works very efficiently when looking for a solution in case that K is not too large (say, for up to $K \approx 20$ points). However, as K increases, the algorithm slows down dramatically. Theoretically, we know that the convergence is

at least linear. Methods requiring the derivative such as Newton's method could not be used in our algorithm since the derivative of the approximated error function is not obvious in our investigation. On the other hand, other procedures that do not need the derivative could speed up the convergence such as applying Nelder-Mead algorithm [18], Powell's method [22], Rosenbrock's method [23] or some other simplex algorithm.

Chapter 2

A Light Beam Reshaping XR System

2.1 Introduction

Optical systems studied so far are generally based on either reflectors (see for example [11], [19], [26]) or refractors (see for example [5], [7], [20] and [21]). In this chapter, a structure involving both a reflector and a refractor will be studied. In optical science, this type of construction is denoted by XR, where X stands for the reflector and R for the refractor. This problem was inspired by the design of a solar energy concentrator by the authors of the book in [29]. These scientists use optical tools and computing software to develop various types of optical devices. To the best of our knowledge, no previous work using our approach to this specific problem has been established so far.

In this chapter, we derive a partial differential equation satisfied by the functions describing the XR system and outline a geometric approach to obtain a possible alternate solution. Although such an equation is obtained in our study, the problem might be approached using other strategies so that one can present more general solutions. One of these strategies, a

geometric approach to the solution using surfaces defined by quadrics, is introduced as well. The reader should keep in mind that this part is a work in progress.

2.2   Description of the System

Let Γ be a plane in $\mathbb{R}^3$ with D and T being two compact subsets of Γ. Without loss of generality, we can consider Γ to be the plane $\{(x_1, x_2, x_3) \in \mathbb{R}^3 : x_3 = 0\}$.

The ray of light initially travels in a medium (Medium I in Figure 2.2) with refractive index n_1 in a vertical upward direction such that it crosses the initial domain $D \subset \Gamma$. The ray reflects off the first surface $\mathcal{R}$ at some point $z \in \mathcal{R}$ and reaches the second surface $\mathcal{L}$. The ray is now refracted parallel to the initial ray in a different medium II with refractive index n_2, and it finally reaches the target domain at some point $p \in T$.
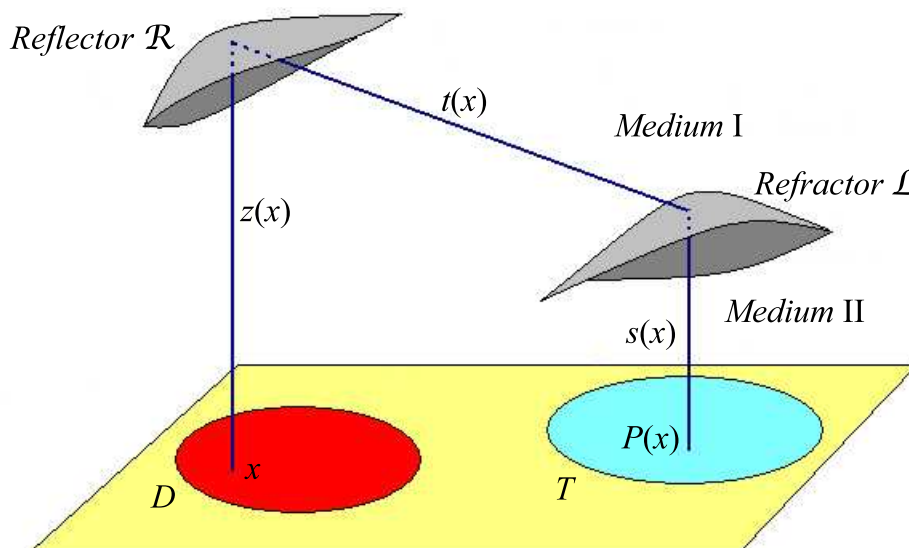

Figure 2.1: Design of the XR system

Given the densities I and L on the domains D and T respectively, the balance condition

$$\int_D I(x)dx = \int_T L(p)dp \tag{2.1}$$

is imposed. This system would then define a mapping $P : D \rightarrow T$ such that $P(x) = p$. Therefore, the problem is to construct a reflector-refractor (XR) system so that the equation

$$I(x) = |J(P(x))| \cdot L(P(x)) \tag{2.2}$$

is satisfied where $J(\cdot)$ stands for the Jacobian matrix operator. Based on these constraints, we would like to describe a system satisfying (2.2).

2.3 Derivation of the PDE

Our goal is to obtain an expression that would describe the map $P : D \rightarrow T$. For simplicity and without loss of generality, we consider the relative refractive index n between the two media (Medium I and Medium II) and define it as $n = \frac{n_2}{n_1}$. The actual optical path length is

$$\tilde{l}(x) = n_1 \cdot z(x) + n_1 \cdot t(x) + n_2 \cdot s(x). \tag{2.3}$$

Then, by dividing both sides by n_1, one gets:

$$l(x) = z(x) + t(x) + n \cdot s(x). \tag{2.4}$$

Now, let $r_1(x) = (x, z(x))$ be the position vector on $\mathcal{R}$ where $z \in C^1(\bar{D})$. The normal vector field on the reflector is

$$\vec{n} = \frac{(-\nabla z, 1)}{\sqrt{1 + |\nabla z|^2}} \tag{2.5}$$

where $\nabla z = \left(\frac{\partial z}{\partial x_1}, \frac{\partial z}{\partial x_2}\right)$. Next, the mapping $p = P(x)$ can be defined as a sum of vectors as follows:

$$P(x) = x + z(x) \cdot \vec{k} + t(x) \cdot \vec{m} + s(x) \cdot \left(-\vec{k}\right) \tag{2.6}$$

where $\vec{m}$ is the direction of the reflected ray and $\vec{k}$ is the vertical upward direction. We can determine the reflected direction $\vec{m}$ using the vector form of the law of reflection $\vec{m} = \vec{k} - 2\langle \vec{k}, \vec{n} \rangle \vec{n}$. Then

$$\vec{m} = \frac{\left(2\nabla z, |\nabla z|^2 - 1\right)}{1 + |\nabla z|^2} \tag{2.7}$$

Once the reflected direction $\vec{m}$ is acquired, we know that the refraction will be in the negative vertical direction, that is, in direction $-\vec{k} = (0,0,-1)$. First, recall that Snell's Law of Refraction implies that a ray obeys the following rule:

$$\sin \theta_1 = n \cdot \sin \theta_2, \tag{2.8}$$

where θ_1 is the angle of incidence and θ_2 is the angle of refraction. Snell's Law also implies that the vector $n_1 \cdot \vec{m} - n_2 \cdot \left(-\vec{k}\right)$ has the same direction as the normal vector $\vec{N}$ to the refracting surface $\mathcal{L}$. Therefore, we can write:

$$\alpha \cdot \vec{N} = \vec{m} + n \cdot \vec{k} \tag{2.9}$$

for some $\alpha \in \mathbb{R}$. Since $\vec{N}$ is a unit vector, it will turn out that

$$\alpha = \langle \vec{m}, \vec{N} \rangle + n \cdot \langle \vec{k}, \vec{N} \rangle \tag{2.10}$$

$$= \cos \theta_1 - n \cdot \cos \theta_2. \tag{2.11}$$

From this, we can get an expression for the second normal vector field on $\mathcal{L}$:

$$\vec{N} = \frac{\vec{m} + n \cdot \vec{k}}{\cos \theta_1 - n \cdot \cos \theta_2} = \frac{\left(2\nabla z, (n+1)|\nabla z|^2 + n - 1\right)}{\left(1 + |\nabla z|^2\right)(\cos \theta_1 - n \cdot \cos \theta_2)}. \tag{2.12}$$

After some simple manipulations, we obtain

$$(\cos \theta_1 - n \cdot \cos \theta_2)^2 = (1 + n^2) + 2n \frac{|\nabla z|^2 - 1}{|\nabla z|^2 + 1}. \tag{2.13}$$

Then, the unit normal vector field on $\mathcal{L}$ can be rewritten as

$$\vec{N} = \frac{\left(2\nabla z, (n+1)\,|\nabla z|^2 + n - 1\right)}{\sqrt{(n^2+1)\left(|\nabla z|^2 + 1\right)^2 + 2n\left(|\nabla z|^4 - 1\right)}}. \tag{2.14}$$

Remark 2.1. *Unlike the case in Chapter 1 for the hyperboloids of revolution (see Theorem 1.6), the unit normal vectors $\vec{n}$ and $\vec{N}$ to the surfaces $\mathcal{R}$ and $\mathcal{L}$ (respectively) corresponding to the same ray are not parallel.*

Let us now go back to the image map $p = P(x)$. We can write it as $P(x) = x + t(x) \cdot \vec{m}_0(x)$ where $\vec{m}_0(x)$ is the projection of the vector $\vec{m}(x)$ onto the plane $z = 0$. Since $\vec{m}_0(x) = \vec{m}(x) - \left\langle \vec{m}(x), \vec{k} \right\rangle \vec{k} = \frac{2\nabla z}{1+|\nabla z|^2}$,

$$P(x) = x + 2t(x)\frac{\nabla z}{1 + |\nabla z|^2}. \tag{2.15}$$

From our construction, it is easy to see that $z(x) = t(x) \cdot \left\langle -\vec{k}, \vec{m}(x) \right\rangle + s(x)$. Let us also impose the constancy of the optical path length by putting $L = z(x) + t(x) + n \cdot s(x)$. Then we get

$$L = (n+1)z(x) + \frac{(n+1)\,|\nabla z|^2 - (n-1)}{1 + |\nabla z|^2}t(x). \tag{2.16}$$

Solving for t, we obtain

$$t(x) = \frac{(L - (n+1)z(x))\left(1 + |\nabla z|^2\right)}{(n+1)\,|\nabla z|^2 - (n-1)}. \tag{2.17}$$

Then the mapping $P(x)$ becomes

$$P(x) = x + 2\frac{L - (n+1)z(x)}{(n+1)\,|\nabla z|^2 - (n-1)}\nabla z. \tag{2.18}$$

Let us introduce some notation by setting

$$K := 2\left(L - (n+1)z\right) \text{ and } Q := (n+1)\,|\nabla z|^2 - (n-1). \tag{2.19}$$

This allows us to write the mapping shortly as follows:

$$P(x) = x + \frac{K}{Q}\nabla z. \tag{2.20}$$

In addition, the refractive surface given by the graph of the function $s = s(p)$ is completely determined by the reflective surface given by the graph of the funciton $z = z(x)$ together with the mapping $p = P(x)$. Since $(p, s) = (x, z) + t(x) \cdot \vec{m}$,

$$s(P(x)) = z(x) + \frac{K}{2Q}\left(|\nabla z|^2 - 1\right). \tag{2.21}$$

We finish this discussion by computing the Jacobian $J(P)$ in the equation (2.2). First, let $x = (x^1, x^2)$ denote a 2-dimensional independent variable. In addition, we want the subscript i to denote the partial derivative with respect to the variable x^i. For example, $z_i := \frac{\partial z}{\partial x^i}$ and $z_{ij} = \frac{\partial^2 z}{\partial x^i \partial x^j}$. Then the mapping P can be expressed in the following way:

$$P(x^1, x^2) := (p^1, p^2) = \left(x^1 + \frac{K}{Q}z_1, x^2 + \frac{K}{Q}z_2\right). \tag{2.22}$$

Therefore, we need to compute

$$|J(P(x))| = \det\begin{pmatrix} A & B \\ C & D \end{pmatrix} = A \cdot D - B \cdot C, \tag{2.23}$$

where $A = \frac{\partial p^1}{\partial x^1}$, $B = \frac{\partial p^1}{\partial x^2}$, $C = \frac{\partial p^2}{\partial x^1}$, $D = \frac{\partial p^2}{\partial x^2}$. Then we obtain the following expressions:

$$
\begin{aligned}
A &= 1 + \frac{K_1}{Q}z_1 + \frac{K}{Q}z_{11} - \frac{K}{Q^2}z_1 Q_1 \\
B &= \frac{K_2}{Q}z_1 + \frac{K}{Q}z_{12} - \frac{K}{Q^2}z_1 Q_2 \\
C &= \frac{K_1}{Q}z_2 + \frac{K}{Q}z_{12} - \frac{K}{Q^2}z_2 Q_1 \\
D &= 1 + \frac{K_2}{Q}z_2 + \frac{K}{Q}z_{22} - \frac{K}{Q^2}z_2 Q_2
\end{aligned}
\tag{2.24}
$$

Here we have that

$$K_i = -2(n+1)z_i \text{ and } Q_i = 2(n+1)(z_1 z_{1i} + z_2 z_{i2}), i = 1, 2. \tag{2.25}$$

Combining the expressions (2.23), (2.24) and (2.25), lengthy but straightforward calculations lead us to the following expression:

$$
\begin{aligned}
|J(P(x))| &= 1 - \frac{2(n+1)}{Q}|\nabla z|^2 + \frac{K}{Q}\triangle z - \frac{2(n+1)K}{Q^2}|\nabla z|^2 \triangle z + \\
&\quad \frac{K^2}{Q^2}\det(z_{ij}) - \frac{2(n+1)K^2}{Q^3}|\nabla z|^2 \det(z_{ij}) \\
&= 1 - \frac{2(n+1)}{Q}|\nabla z|^2 + \frac{K}{Q}\triangle z\left(1 - \frac{2(n+1)}{Q}|\nabla z|^2\right) + \tag{2.26} \\
&\quad \frac{K^2}{Q^2}\det(z_{ij})\left(1 - \frac{2(n+1)}{Q}|\nabla z|^2\right) \\
&= \left(1 - \frac{2(n+1)}{Q}|\nabla z|^2\right)\left(1 + \frac{K}{Q}\triangle z + \frac{K^2}{Q^2}\det(z_{ij})\right),
\end{aligned}
$$

where $\det(z_{ij})$ stands for the determinant of the matrix of second-order partial derivatives of the function $z = z(x), x \in D$. To permit further simplifications, let $\xi = \frac{Q}{K}$ so that the expression in (2.26) can be written as:

$$|J(P)| = \frac{1}{\xi^2}\frac{(n-1) + (n+1)|\nabla z|^2}{(n-1) - (n+1)|\nabla z|^2}\left(\xi^2 + \xi\triangle z + \det(z_{ij})\right). \tag{2.27}$$

After final rearrangements of terms and by putting $\gamma = \frac{n-1}{n+1}$, the PDE (2.2) can be established as follows:

$$I(x) = \frac{1}{\xi^2}\frac{\gamma + |\nabla z|^2}{\gamma - |\nabla z|^2}\det\left(z_{ij} + \delta_{ij}\xi\right) \cdot L\left(P(x)\right), \tag{2.28}$$

where $P(x)$ is given in (2.20), $\xi = \frac{(n-1) - (n+1)|\nabla z|^2}{2[(n+1)z - (n-1)]}$ and δ_{ij} is the Kronecker delta.

2.4 A Geometric Approach to the XR Problem

2.4.1 Introduction

In the previous section, we derived explicit expressions for both the mapping $P : D \to T$ and the PDE of the XR problem. In this section, we formulate expressions describing surfaces z and s in the XR system by looking at the problem from a geometric point of view.

In our construction, we use the definition of convex bodies in $\mathbb{R}^3$ that is based on the idea of the intersection of families of half-spaces. In our case, instead of half-spaces, we use branches of hyperboloids of revolution and ellipsoids of revolution.

Our approach is similar to that used in [6], [9] and [21]. The requirement that the optical path length be constant defines families of quadrics. These quadrics have special reflecting and refracting properties that make the connection between the two surfaces in the XR system. Next, applying the inf and sup operators, we obtain the required surfaces solving the problem. Note that the surfaces obtained need not be smooth. However, this particular approach permits the definition of a geometric variant of the mapping $P : D \to T$ given in (2.20). Future plans on this problem involve the establishment of weak solutions of the XR problem, together with the proofs of the existence and uniqueness of the solution.

2.4.2 The XR Surfaces

First, let us recall the OPL of the system:

$$L = z(x) + \sqrt{|x - p|^2 + (z(x) - s(p))^2} + n \cdot s(p) \text{ where } x \in D, p \in T. \quad (2.29)$$

Solving for the variables z and s separately, we can express z in terms of s and vice versa.

Let us begin with the surface $z = F(x, p, s(p))$. The terms of the equation in (2.29) can be rearranged to get:

$$(L - (n-1)s - 2z)(L - (n+1)s) = |x - p|^2.$$ (2.30)

This in turn leads us to the formulation:

$$z = \frac{1}{2}\left(L - (n-1)s - \frac{|x-p|^2}{L - (n+1)s}\right).$$ (2.31)

Lemma 2.2. *For any fixed (p, s), the surface $z = \mathcal{P}_{p,s}(x)$ given by the equation (2.31) is a paraboloid of revolution with vertex at $\left(p, \frac{L-(n-1)s}{2}\right)$ and focus located at the point $F_p = (p, s)$. The focal parameter will be $p_f = (n+1)s - L$.*

Proof. We simply need to write (2.31) in the quadric form $|x - x_0|^2 = 4a(z - z_0)$:

$$|x - p|^2 = 4\left(\frac{(n+1)s - L}{2}\right)\left(z - \frac{L - (n-1)s}{2}\right).$$ (2.32)

This is the equation for the paraboloid of revolution with vertical axis through $\left(p, \frac{L-(n-1)s}{2}\right)$, which is the vertex of the paraboloid. The focus is located at $F_p = \left(p, \frac{L-(n-1)s}{2} - |a|\right)$ where $a = \frac{(n+1)s - L}{2}$. The focal parameter is $p_f = 2|a| = (n+1)s - L$. $\qquad \square$

On the other hand, solving the equation (2.29) for the variable s, we obtain an equation $s = G(x, p, z(x))$ given by the following pair of surfaces:

$$s = \frac{1}{n^2 - 1}\left(nL - (n+1)z \pm \sqrt{(L - (n+1)z)^2 + (n^2 - 1)|x - p|^2}\right).$$ (2.33)

Lemma 2.3. *Let (x, z) be fixed.*

- *If $n > 1$, the surface given by the equation (2.33) is a two-sheeted hyperboloid of revolution centered at $\left(x, \frac{nL-(n+1)z}{n^2-1}\right)$ with upper focus $F^+ = (x, z)$ and lower focus $F^- = \left(x, \frac{2nL-(n+1)^2z}{n^2-1}\right)$, and with eccentricity $e = n$.*

- *If $0 < n < 1$, the surface given by the equation (2.33) is an ellipsoid of revolution centered at $\left(x, \frac{nL-(n+1)z}{n^2-1}\right)$ with upper focus $F^+ = (x, z)$ and lower focus $F^- = \left(x, \frac{2nL-(n+1)^2z}{n^2-1}\right)$, and with eccentricity $e = n$.*

Remark 2.4. *In both cases, only the lower halves of these surfaces will be considered in our constructions. Therefore, we will denote by $s = \mathcal{H}_{x,z}(p)$ the lower branch of the two-sheeted hyperboloid of revolution for the case $n > 1$ and by $s = \mathcal{E}_{x,z}(p)$ the lower half of the ellipsoid of revolution when $0 < n < 1$.*

Proof. We need to rewrite the equation (2.33) in the following form:

$$\frac{\left(s - \frac{\beta+(n-1)L}{n^2-1}\right)^2}{\frac{\beta^2}{(n^2-1)^2}} - \frac{\left|p - x\right|^2}{\frac{\beta^2}{n^2-1}} = 1 \tag{2.34}$$

where $\beta = L - (n+1)z$. This is obviously the general equation for the two-sheeted hyperboloid of revolution with center at $\left(x, \frac{nL-(n+1)z}{n^2-1}\right)$. The eccentricity can easily be computed using the formula $e = \sqrt{1 + \frac{b^2}{a^2}}$ where $a = \frac{\beta}{n^2-1}$ and $b = \frac{\beta}{\sqrt{n^2-1}}$. $\square$

The following lemma is a statement of the well-known fact that any ray of light parallel to the axis of a paraboloid is reflected so as to pass through the focus.

Lemma 2.5. *Fix the point $(p, s) \in T \times \mathbb{R}$. Then for each $x \in D$, the ray through x in positive vertical direction reflects at $(x, \mathcal{P}_{p,s}(x))$. All such reflected rays pass through the focus $F_p = (p, s)$.*

The following lemma is based on Snell's Law of Refraction and is due to Descartes. It can be verified using simple properties of conics. The proof will be omitted here and the reader should refer to the discussion in [16] for details.

Lemma 2.6. • *Let $n > 1$ and the point $(x, z) \in D \times \mathbb{R}$ be fixed. Then if the lower branch of the hyperboloid $s(p) = \mathcal{H}_{x,z}(p)$ with eccentricity $e = n$ is constructed of material of refractive index n, rays of light parallel to the major axis (vertical upwards) will be refracted so as to pass through the upper focus $F^+ = (x, z)$. The opposite direction holds true as well. That is, rays passing through the upper focus $F^+ = (x, z)$ and hitting the surface of the lower branch of the hyperboloid will be refracted so as to have a direction parallel to the major axis of the hyperboloid (vertical downwards).*

• *Let $0 < n < 1$ and the point $(x, z) \in D \times \mathbb{R}$ be fixed. Then if the lower half of the ellipsoid of revolution $s(p) = \mathcal{E}_{x,z}(p)$ with eccentricity $e = n$ is constructed of material of refractive index n, rays of light parallel to the major axis (vertical upwards) will be refracted so as to pass through the upper focus $F^+ = (x, z)$. The opposite direction holds true as well. That is, rays passing through the upper focus $F^+ = (x, z)$ and hitting the surface of the lower branch of the ellipsoid of revolution will be refracted so as to have a direction parallel to the major axis of the ellipsoid (vertical downwards).*

Lemmas 2.5 and 2.6 have been combined and illustrated in Figures 2.2 and 2.3 for the two cases when $n > 1$ and $0 < n < 1$, respectively. In both cases, the ray initiated at the point $x \in D$ and moving in the vertical direction up to the surface $s = \mathcal{P}_{x,z}$ (reflector) reaches the point (x, z), which is in the meantime the focus associated to the lower half of the refractor. Here, the ray is reflected off towards the focus of the paraboloid, which in turn is located on the surface of the refractor (either $z = \mathcal{H}_{p,s}(x)$ if $n > 1$ or $z = \mathcal{E}_{p,s}(x)$ if $0 < n < 1$). At this point, the ray is refracted and continues its trajectory in the negative vertical direction and finally reaches the target point $p \in T$.

The discussion above can be summarized in the following corollary. This is the main key to defining the XR system as envelopes of families of
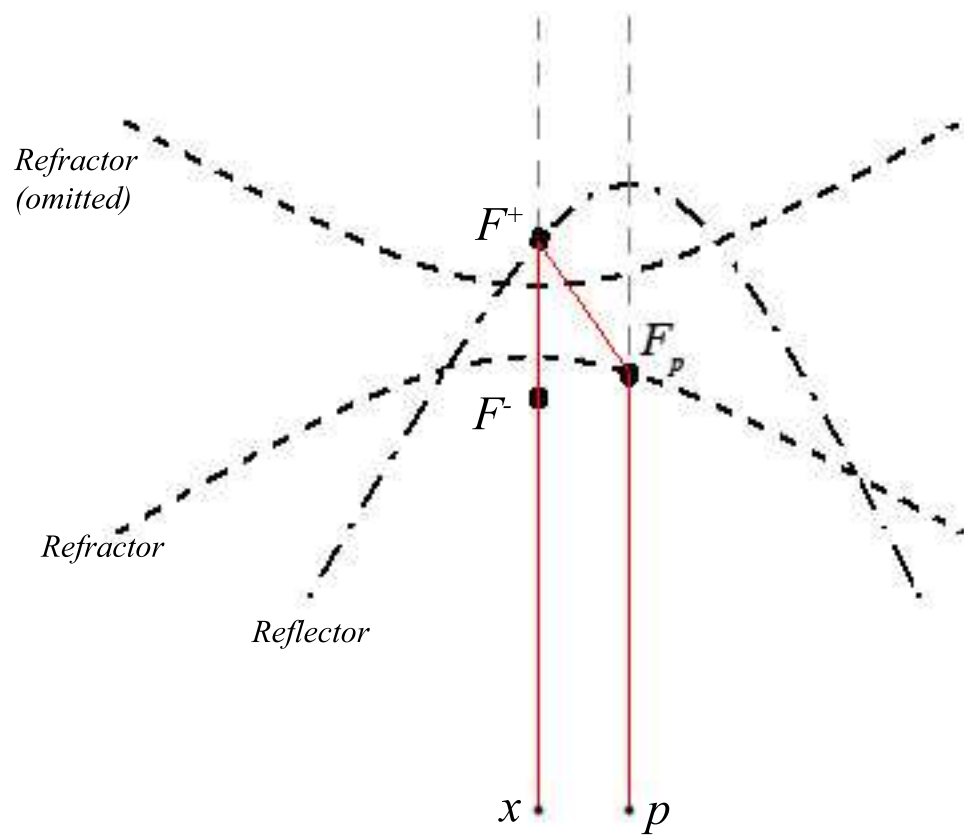
Figure 2.2: Case I: $n > 1$. Here, the ray issued at x in the vertical up-
ward direction is reflected off at $F^+ = (x, z)$ in direction of the focus of the
paraboloid. The ray then reaches the point $F_p = (p, s)$, where it is refracted
in the negative vertical direction, since it reflected off at F^+, which is the
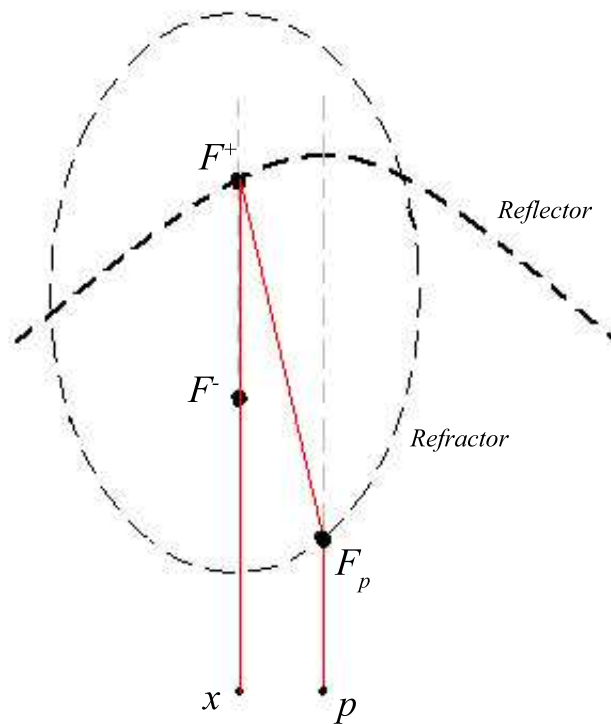upper focus of the hyperboloid associated to the lower branch.

Figure 2.3: Case II: $0 < n < 1$. This time, the ray issued at x in the vertical upward direction is reflected off at $F^+ = (x, z)$ in direction of the focus F_p of the paraboloid. Again, the ray reaches the point $F_p = (p, s)$, where it is refracted in the negative vertical direction since it reflected off at F^+, which is the upper focus of the ellipsoid of revolution.

quadrics. These quadrics will be either a paraboloid with a branch of a hyperboloid of revolution if $n > 1$ or a paraboloid with an ellipsoid of revolution if $0 < n < 1$. Recall that $\mathcal{R}$ (reflector) and $\mathcal{L}$ (refractor) are the two surfaces of the XR optical system as in Section 2.3.

Corollary 2.7. *Let $\mathcal{R}$ and $\mathcal{L}$ be the graphs defined by two functions $z \in C^1(\bar{D})$ and $s \in C^1(\bar{T})$, respectively. Assume also that the XR mapping $P : \bar{D} \to \bar{T}$ is a diffeomorphism. In addition, fix some point $(x_0, z(x_0)) \in \mathcal{R}$ and let $(p_0, s(p_0)) \in \mathcal{L}$ where $p_0 = P(x_0)$.*

1. *$z(x_0) = \mathcal{P}_{p_0, s(p_0)}(x_0)$, where $\mathcal{P}_{p_0, s(p_0)}$ is the paraboloid of revolution with vertical axis of symmetry and focus at $F_p = (p_0, s(p_0))$. Moreover, the hyperplanes tangent to $\mathcal{R}$ at $(x_0, z(x_0))$ and to the graph of $z = \mathcal{P}_{p_0, s(p_0)}$ at x_0 coincide.*

2. (a) *If $n > 1$, $s(p_0) = \mathcal{H}_{x_0, z(x_0)}(x_0)$, where $\mathcal{H}_{x_0, z(x_0)}$ is the lower branch of a hyperboloid of revolution with vertical major axis and corresponding focus $F^+ = (x_0, z(x_0))$. Moreover, the hyperplanes tangent to $\mathcal{L}$ at $(p_0, s(p_0))$ and to the graph of $s = \mathcal{H}_{x_0, z(x_0)}$ at p_0 coincide.*

   (b) *If $0 < n < 1$, $s(p_0) = \mathcal{E}_{x_0, z(x_0)}(x_0)$, where $\mathcal{E}_{x_0, z_0}$ is the lower half of an ellipsoid of revolution with vertical major axis and corresponding focus $F^+ = (x_0, z(x_0))$. Moreover, the hyperplanes tangent to $\mathcal{L}$ at $(p_0, s(p_0))$ and to the graph of $s = \mathcal{E}_{x_0, z(x_0)}$ at p_0 coincide.*

2.5 Conclusion

In this chapter, we introduced an XR system that involves both a mirror and a lens. Clearly, our work is still in progress and the achievements in this problem are far for complete. Our future work plans include, but are not restricted to the derivation of the theorems for the existence and

uniqueness of the solution to the XR problem together with the formation of weak and variational solutions to the XR problem. The method presented in this chapter should be applicable to RX systems as well, where light rays first refract through a lens and then reflect off a mirror. In addition, we claim that the XR problem could be studied for the case of light issued at a point source instead of a collimated beam. We also believe that an analogue of the numerical method presented in Chapter 1 would be interesting to investigate.

Chapter 3

A Collimated Source Problem

3.1   Introduction

In this chapter, we discuss a reflector problem previously introduced in [11]. This section has great importance in our whole dissertation as it involves detailed derivations of equations. Similar methods are used in Chapter 2 where some of the details are skipped there.

We first describe the problem, then derive the partial differential equation (PDE) related to this problem. It was shown in [11] that this PDE is of Monge-Ampère type. Next we consider the rotationally symmetric case of the setup and give the equation related to it, which is an ordinary differential equation (ODE). Finally we illustrate the discussion by defining a numerical example.

3.2   Description of the Problem

The problem can be presented as follows. Consider a collimated beam of light emitted in the vertical upward direction. Let $D \subset \mathbb{R}^2$ be the intersection of this beam with the plane $\mathbb{R}^2 = \{(x, y, z : z = 0)\}$ in 3-dimensional space. Let T be another domain on the same plane $\mathbb{R}^2$. Let $I = I(x, y), (x, y) \in$

D be the intensity of the light over the domain D and $L = L(\alpha, \beta)$ be the intensity of the light on T. Now consider a reflector $\mathcal{R}$ (some surface in $\mathbb{R}^3$) lying above the domain D. The rays passing through D will hit and reflect off the reflector $\mathcal{R}$ and reach the target domain T (See Figure 3.1). Both I and L are considered to be integrable functions.
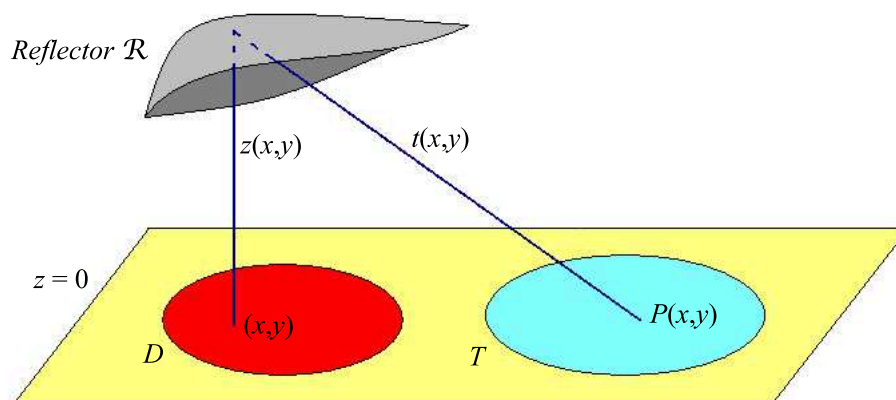

Figure 3.1: Design of the problem

Then, we can say that the reflector $\mathcal{R}$ actually defines a map $\gamma : D \longrightarrow T$ with

$$\gamma(x, y) = (\alpha(x, y), \beta(x, y)).$$

The problem is to construct such a surface that satisfies the following PDE:

$$I(x, y) = \left| J(\gamma(x, y)) \right| \cdot L(\gamma(x, y)) \tag{3.1}$$

where J stands for the Jacobian.

We want to describe an explicit form of:

1. the map γ

2. its Jacobian $J(\gamma(\cdot, \cdot))$

3. the equation (3.1)

with no assumption regarding the symmetry of D, T, I and L.

3.3   The Derivation of the PDE

Let $z = z(x, y)$ be a function defined over the domain D and giving the vertical distance between the point $(x, y) \in D$ and $(x, y, z) \in \mathcal{R}$. The two vectors

$$\left(1, 0, \frac{\partial z}{\partial x}\right) \text{ and } \left(0, 1, \frac{\partial z}{\partial y}\right) \tag{3.2}$$

are orthogonal and tangent to the surface $\mathcal{R}$ at (x, y, z). Then, the unit normal vector will be

$$\vec{n} = \frac{\left(1, 0, \frac{\partial z}{\partial x}\right) \times \left(0, 1, \frac{\partial z}{\partial y}\right)}{\left|\left(1, 0, \frac{\partial z}{\partial x}\right) \times \left(0, 1, \frac{\partial z}{\partial y}\right)\right|} = \frac{\left(-\frac{\partial z}{\partial x}, -\frac{\partial z}{\partial y}, 1\right)}{\sqrt{\left(\frac{\partial z}{\partial x}\right)^2 + \left(\frac{\partial z}{\partial y}\right)^2 + 1}} = \frac{(-\nabla z, 1)}{\sqrt{|\nabla z|^2 + 1}} \tag{3.3}$$

where $\nabla z = \left(\frac{\partial z}{\partial x}, \frac{\partial z}{\partial y}\right)$. Let $\vec{m} = (0, 0, 1)$ be the direction of the emitted light. We can find the direction $\vec{b}$ of the reflected light using the formula

$$\vec{b} = \vec{m} - 2\langle \vec{m}, \vec{n}\rangle \vec{n}.$$

Therefore, the reflected direction will be:

$$\vec{b} = \frac{\left(2\nabla z, |\nabla z|^2 - 1\right)}{|\nabla z|^2 + 1}. \tag{3.4}$$

Note that $\left|\vec{b}\right| = 1$.

Suppose that $t(x, y)$ is the distance between the points $(x, y, z) \in \mathcal{R}$ and $(\alpha, \beta, 0) \in T$. Then we have:

$$t(x, y) = \frac{z(x, y)}{\langle -m, b\rangle} = \frac{1 + |\nabla z|^2}{1 - |\nabla z|^2} z(x, y). \tag{3.5}$$

Therefore, we can deduce the mapping $\gamma = \gamma(x, y)$ as follows:

$$
\begin{aligned}
(\alpha, \beta, 0) = \gamma(x, y) &= (x, y, 0) + z(x, y) \cdot \vec{m} + t(x, y) \cdot \vec{b} \\
&= (x, y, 0) + z \cdot (0, 0, 1) + \frac{1 + |\nabla z|^2}{1 - |\nabla z|^2} z \cdot \frac{\left(2\frac{\partial z}{\partial x}, 2\frac{\partial z}{\partial y}, |\nabla z|^2 - 1 \right)}{|\nabla z|^2 + 1} \\
&= (x, y, 0) + (0, 0, z) + z \cdot \left(\frac{2\frac{\partial z}{\partial x}}{1 - |\nabla z|^2}, \frac{2\frac{\partial z}{\partial y}}{1 - |\nabla z|^2}, -1 \right) \quad (3.6) \\
&= (x, y, 0) + \left(\frac{2z\frac{\partial z}{\partial x}}{1 - |\nabla z|^2}, \frac{2z\frac{\partial z}{\partial y}}{1 - |\nabla z|^2}, 0 \right).
\end{aligned}
$$

As a result, we can write this in a shorter form:

$$
\gamma(x, y) = (\alpha, \beta) = (x, y) + \frac{2z(x, y)}{1 - |\nabla z|^2} \nabla z. \quad (3.7)
$$

Next, we can compute the Jacobian of γ. We have that

$$
\alpha(x, y) = x + \frac{2z}{1 - |\nabla z|^2} \frac{\partial z}{\partial x} \quad \text{and} \quad \beta(x, y) = y + \frac{2z}{1 - |\nabla z|^2} \frac{\partial z}{\partial y}. \quad (3.8)
$$

So,

$$
\begin{aligned}
A &:= \frac{\partial \alpha}{\partial x} = 1 + \frac{\partial}{\partial x} \left(\frac{2z}{1 - |\nabla z|^2} \frac{\partial z}{\partial x} \right) \\
B &:= \frac{\partial \alpha}{\partial y} = \frac{\partial}{\partial y} \left(\frac{2z}{1 - |\nabla z|^2} \frac{\partial z}{\partial x} \right) \\
C &:= \frac{\partial \beta}{\partial x} = \frac{\partial}{\partial x} \left(\frac{2z}{1 - |\nabla z|^2} \frac{\partial z}{\partial y} \right) \quad (3.9) \\
D &:= \frac{\partial \beta}{\partial y} = 1 + \frac{\partial}{\partial y} \left(\frac{2z}{1 - |\nabla z|^2} \frac{\partial z}{\partial y} \right).
\end{aligned}
$$

Now we compute these components. We know that

$$
\left| J(\gamma(x, y)) \right| = A \cdot D - B \cdot C \quad (3.10)
$$

For simplicity, let us introduce the following notation:

$$z_1 = \frac{\partial z}{\partial x}; \qquad z_2 = \frac{\partial z}{\partial y};$$
$$z_{11} = \frac{\partial^2 z}{\partial x^2}; \qquad z_{22} = \frac{\partial^2 z}{\partial y^2}; \tag{3.11}$$
$$z_{12} = z_{21} = \frac{\partial^2 z}{\partial x \partial y}.$$

We will need:

$$\frac{\partial}{\partial x}\left(|\nabla z|^2\right) = \frac{\partial}{\partial x}\left((z_1)^2 + (z_2)^2\right) = 2z_1 z_{11} + 2z_2 z_{12}$$

and

$$\frac{\partial}{\partial y}\left(|\nabla z|^2\right) = \frac{\partial}{\partial y}\left((z_1)^2 + (z_2)^2\right) = 2z_1 z_{12} + 2z_2 z_{22}.$$

So, we get:

$$
\begin{aligned}
A & = \frac{\partial \alpha}{\partial x} = 1 + \frac{\partial}{\partial x}\left(\frac{2z}{1 - |\nabla z|^2}\frac{\partial z}{\partial x}\right) \\
& = 1 + \frac{2}{1 - |\nabla z|^2}(z_1)^2 + \frac{2z}{1 - |\nabla z|^2}z_{11} + 2zz_1\frac{\partial}{\partial x}\left(\frac{1}{1 - |\nabla z|^2}\right) \tag{3.12} \\
& = 1 + \frac{2}{1 - |\nabla z|^2}(z_1)^2 + \frac{2z}{1 - |\nabla z|^2}z_{11} + \frac{4z}{(1 - |\nabla z|^2)^2}z_1(z_1 z_{11} + z_2 z_{12}).
\end{aligned}
$$

Similarly, we arrive at:

$$D = 1 + \frac{2}{1 - |\nabla z|^2}(z_2)^2 + \frac{2z}{1 - |\nabla z|^2}z_{22} + \frac{4z}{(1 - |\nabla z|^2)^2}z_2(z_1 z_{12} + z_2 z_{22}). \tag{3.13}$$

Also, we have:

$$
\begin{aligned}
B & = \frac{\partial \alpha}{\partial y} = \frac{\partial}{\partial y}\left(\frac{2z}{1 - |\nabla z|^2}\frac{\partial z}{\partial x}\right) \\
& = \frac{2}{1 - |\nabla z|^2}z_1 z_2 + \frac{2z}{1 - |\nabla z|^2}z_{12} + 2zz_1\frac{\partial}{\partial y}\left(\frac{1}{1 - |\nabla z|^2}\right) \tag{3.14} \\
& = \frac{2}{1 - |\nabla z|^2}z_1 z_2 + \frac{2z}{1 - |\nabla z|^2}z_{12} + \frac{4z}{(1 - |\nabla z|^2)^2}z_1(z_1 z_{12} + z_2 z_{22}).
\end{aligned}
$$

In a similar manner, we write:

$$C = \frac{2}{1 - |\nabla z|^2}z_1 z_2 + \frac{2z}{1 - |\nabla z|^2}z_{12} + \frac{4z}{(1 - |\nabla z|^2)^2}z_2(z_1 z_{11} + z_2 z_{12}). \tag{3.15}$$

Therefore,

$$
\begin{aligned}
\left| J(\gamma) \right| &= A \cdot D - B \cdot C \\
&= 1 + \frac{2}{1 - |\nabla z|^2} \left((z_1)^2 + (z_2)^2 \right) + \frac{2z}{1 - |\nabla z|^2} (z_{11} + z_{22}) \\
&\quad + \frac{4z}{(1 - |\nabla z|^2)^2} \left((z_1)^2 z_{22} + (z_1)^2 z_{11} + (z_2)^2 z_{11} + (z_2)^2 z_{22} \right) \\
&\quad + \frac{4z^2}{(1 - |\nabla z|^2)^2} \left(z_{11} z_{22} - (z_{12})^2 \right) \\
&\quad + \frac{8z^2}{(1 - |\nabla z|^2)^3} \left((z_1)^2 z_{11} z_{22} + (z_2)^2 z_{11} z_{22} - (z_1)^2 (z_{12})^2 - (z_2)^2 (z_{12})^2 \right) \quad (3.16) \\
&= 1 + \frac{2 |\nabla z|^2}{1 - |\nabla z|^2} + \frac{2z}{1 - |\nabla z|^2} \triangle z + \frac{4z}{(1 - |\nabla z|^2)^2} |\nabla z|^2 \triangle z \\
&\quad + \frac{4z^2}{(1 - |\nabla z|^2)^2} \det(z_{ij}) + \frac{8z^2}{(1 - |\nabla z|^2)^3} |\nabla z|^2 \det(z_{ij}) \\
&= \frac{1 + |\nabla z|^2}{1 - |\nabla z|^2} + \frac{2z(1 + |\nabla z|^2)}{(1 - |\nabla z|^2)^2} \triangle z + \frac{4z^2(1 + |\nabla z|^2)}{(1 - |\nabla z|^2)^3} \det(z_{ij}).
\end{aligned}
$$

Now, putting $\eta := \frac{1 - |\nabla z|^2}{2z}$, we can write this Jacobian in a simpler form:

$$
\begin{aligned}
J(\gamma) &= \frac{1 + |\nabla z|^2}{1 - |\nabla z|^2} + \frac{(1 + |\nabla z|^2)}{\eta(1 - |\nabla z|^2)} \triangle z + \frac{1 + |\nabla z|^2}{\eta^2(1 - |\nabla z|^2)} \det(z_{ij}) \\
&= \frac{1}{\eta^2} \frac{1 + |\nabla z|^2}{1 - |\nabla z|^2} \left(\eta^2 + \eta \triangle z + \det(z_{ij}) \right) \\
&= \frac{1}{\eta^2} \frac{1 + |\nabla z|^2}{1 - |\nabla z|^2} \left(\eta^2 + \eta z_{11} + \eta z_{22} + z_{11} z_{22} - (z_{12})^2 \right) \\
&= \frac{1}{\eta^2} \frac{1 + |\nabla z|^2}{1 - |\nabla z|^2} \left((z_{11} + \eta)(z_{22} + \eta) - (z_{12})^2 \right) \quad (3.17) \\
&= \frac{1}{\eta^2} \frac{1 + |\nabla z|^2}{1 - |\nabla z|^2} \det \begin{pmatrix} z_{11} + \eta & z_{12} \\ z_{21} & z_{22} + \eta \end{pmatrix} \\
&= \frac{1}{\eta^2} \frac{1 + |\nabla z|^2}{1 - |\nabla z|^2} \det(z_{ij} + \delta_{ij} \eta)
\end{aligned}
$$

where δ_{ij} is the Kronecker delta.

As a result, we can write the PDE (3.1) as follows:

$$I(x, y) = \left| \det(z_{ij} + \delta_{ij}\eta) \frac{1 + |\nabla z|^2}{1 - |\nabla z|^2} \frac{1}{\eta^2} \right| L(\alpha, \beta). \qquad (3.18)$$

3.4   The Rotationally Symmetric Case

Given the PDE (3.18) with $\eta = \frac{1 - |\nabla|^2}{2z}$ and $|\nabla z| < 1$, let us assume that $L \equiv 1$ on the set $T = \{(\alpha, \beta) \in \mathbb{R}^2 | (\alpha, \beta) = \Gamma(x, y)\}$. Set $z = z(r) = z\left(\sqrt{x^2 + y^2} \right)$. So, $r^2 = x^2 + y^2$ and

$$\frac{\partial r}{\partial x} = \frac{x}{r} \text{ and } \frac{\partial r}{\partial y} = \frac{y}{r}. \qquad (3.19)$$

We need the following first and second order partial derivatives:

$$
\begin{aligned}
z_x &= z_r r_x = \frac{x}{r} z_r \\
z_y &= z_r r_y = \frac{y}{r} z_r \\
z_{xx} &= \frac{1}{r} z_r - \frac{x^2}{r^3} z_r + \frac{x^2}{r^2} z_{rr} \\
z_{yy} &= \frac{1}{r} z_r - \frac{y^2}{r^3} z_r + \frac{y^2}{r^2} z_{rr} \\
z_{xy} = z_{yx} &= \frac{xy}{r^2} z_{rr} - \frac{xy}{r^3} z_r.
\end{aligned}
\qquad (3.20)
$$

Then, we can compute $|\nabla z|^2$ and $\triangle z$.

$$
\begin{aligned}
|\nabla z|^2 &= \left(\frac{\partial r}{\partial x} \right)^2 + \left(\frac{\partial r}{\partial y} \right)^2 = \left(\frac{x}{r} z_r \right)^2 + \left(\frac{y}{r} z_r \right)^2 \\
&= \frac{x^2 + y^2}{r^2} (z_r)^2.
\end{aligned}
\qquad (3.21)
$$

Then,

$$|\nabla z|^2 = (z_r)^2. \qquad (3.22)$$

Also,

$$
\begin{aligned}
\Delta z &= z_{xx} + z_{yy} \\
&= \frac{1}{r}z_r - \frac{x^2}{r^3}z_r + \frac{x^2}{r^2}z_{rr} + \frac{1}{r}z_r - \frac{y^2}{r^3}z_r + \frac{y^2}{r^2}z_{rr} \\
&= \frac{2}{r}z_r - \frac{x^2+y^2}{r^3}z_r + \frac{x^2+y^2}{r^2}z_{rr}.
\end{aligned}
\tag{3.23}
$$

Then, we have the Laplacian:

$$
\Delta z = \frac{1}{r}z_r + z_{rr}.
\tag{3.24}
$$

We can now compute the determinant $\det(z_{ij} + \delta_{ij}\eta)$.

$$
\begin{aligned}
\det(z_{ij} + \delta_{ij}\eta) &= \begin{vmatrix} z_{11} + \eta & z_{12} \\ z_{21} & z_{22} + \eta \end{vmatrix} \\
&= z_{xx}z_{yy} + \eta(z_{xx} + z_{yy}) + \eta^2 - (z_{xy})^2 \\
&= \left(\frac{1}{r}z_r - \frac{x^2}{r^3}z_r + \frac{x^2}{r^2}z_{rr}\right)\left(\frac{1}{r}z_r - \frac{y^2}{r^3}z_r + \frac{y^2}{r^2}z_{rr}\right) \\
&\quad + \eta\left(\frac{1}{r}z_r + z_{rr}\right) + \eta^2 - \left(\frac{xy}{r^2}z_{rr} - \frac{xy}{r^3}z_r\right)^2 \\
&= \left(\frac{1}{r^2} - \frac{x^2}{r^4} - \frac{y^2}{r^4}\right)z_r^2 + \left(\frac{x^2}{r^3} + \frac{y^2}{r^3}\right)z_r z_{rr} \\
&\quad + \frac{1 - z_r^2}{2z}\left(\frac{1}{r}z_r + z_{rr}\right) + \left(\frac{1 - z_r^2}{2z}\right)^2.
\end{aligned}
\tag{3.25}
$$

Therefore,

$$
\det z_{ij} + \delta_{ij}\eta = \frac{1}{r}z_r z_{rr} + \frac{1 - z_r^2}{2z}\left(\frac{1}{r}z_r + z_{rr}\right) + \left(\frac{1 - z_r^2}{2z}\right)^2.
\tag{3.26}
$$

Together with the remaining piece of the Jacobian in equation (3.18),

$$
\frac{1 + |\nabla z|^2}{1 - |\nabla z|^2}\frac{1}{\eta^2} = \frac{4z^2(1 + z_r^2)}{(1 - z_r^2)^3}
$$

we get the following second-order nonlinear ODE:

$$I(r) = \left[\frac{1}{r}z_r z_{rr} + \frac{1-z_r^2}{2z}\left(\frac{1}{r}z_r + z_{rr}\right) + \left(\frac{1-z_r^2}{2z}\right)^2\right]\frac{4z^2(1+z_r^2)}{(1-z_r^2)^3}. \tag{3.27}$$

Since $\nabla z = z_r$, we can also obtain the map $\gamma = \gamma(r)$ from (3.7):

$$\gamma(r) = r + \frac{2z}{1-z_r^2}z_r \tag{3.28}$$

We want to solve the ODE (3.27) numerically using MATLAB. To do that, we have to write it as a system of first-order ODE's so that we can use the ODE solver `ode45` in MATLAB. Let us put

$$\begin{cases} Z_1 := z \\ Z_2 := z_r \end{cases} \tag{3.29}$$

Then, we can transform (3.27) into a system of ODE's of the following form:

$$\begin{cases} Z_1' = Z_2 \\ Z_2' = F(r, Z_1, Z_2). \end{cases} \tag{3.30}$$

Therefore, the ODE (3.27) can be rewritten as follows:

$$\begin{aligned} Z_1' &= Z_2 \\ Z_2' &= \frac{I(r)\frac{(1-Z_2^2)^3}{1+Z_2^2} - (1-Z_2^2)^2 - \frac{2}{r}Z_1 Z_2(1-Z_2^2)}{\frac{4}{r}Z_1^2 Z_2 + 2Z_1(1-Z_2^2)} \end{aligned} \tag{3.31}$$

3.5 An Example

Consider the following density function on D:

$$I(x,y) = c \cdot \exp\left(-\frac{x^2+y^2}{2\sigma^2}\right) \tag{3.32}$$

where σ is a parameter and c is a balancing constant (to be determined) enforcing the energy conservation. We define the domains D and T as:

$$D = \left\{(x, y) \in \mathbb{R} : x^2 + y^2 \le (3\sigma)^2\right\} \tag{3.33}$$

and

$$T = \left\{(\alpha, \beta) \in \mathbb{R} : \alpha^2 + \beta^2 \le (2\sigma)^2\right\}. \tag{3.34}$$

We have already assumed the uniform density over T as $L \equiv 1$. Let us now determine the balancing constant c. We need to have:

$$\iint_D I(x, y)dxdy = \iint_T L(\alpha, \beta)d\alpha d\beta. \tag{3.35}$$

Clearly, $\iint_T LdA = 4\pi\sigma^2$. Using the method of cylindrical shells,

$$\begin{aligned} J := \iint_D Idxdy &= c \int_0^{3\sigma} 2\pi r e^{-\frac{r^2}{2\sigma^2}} dr \tag{3.36} \\ &= c2\sqrt{2}\sigma\pi\left(1 - \frac{1}{e^{9/4}}\right). \end{aligned}$$

Due to the conservation of energy (3.35), we must have $J = 4\pi\sigma^2$. Thus, the constant c turns out to be:

$$c = c(\sigma) = \frac{\sqrt{2}\sigma}{1 - \frac{1}{e^{9/4}}}. \tag{3.37}$$

Therefore, the density that satisfies the energy conservation must be

$$I_\sigma(x, y) = \frac{\sqrt{2}\sigma}{1 - \frac{1}{e^{9/4}}} \exp\left(-\frac{x^2 + y^2}{2\sigma^2}\right). \tag{3.38}$$

Let the value z_0 refer to the initial condition of the problem. Below we illustrate the numerical solution, which gives parabola-like shaped surfaces.

In Figure 3.2, we use several different values for the parameter σ; namely $\sigma = 0.125$, $\sigma = 0.25$ and $\sigma = 0.375$. This changes the radius of the initial domain as well as the shape of the distribution although the total intensity remains constant. We keep the initial value $z_0 = 2.0$ fixed in order to compare the different surfaces generated for different parameters. The superposition of all these three surfaces is presented in Figure 3.5.

(a) Parameter value: $\sigma = 0.125$

(b) Paramter value: $\sigma = 0.25$
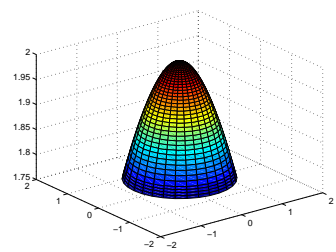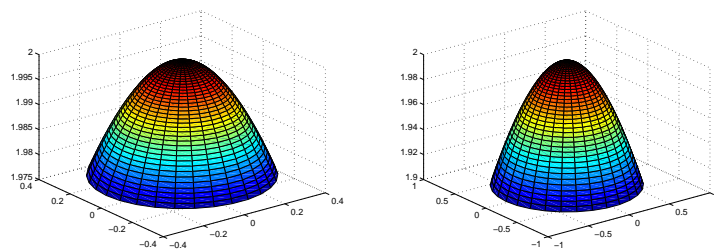
(c) Paramter value: $\sigma = 0.375$

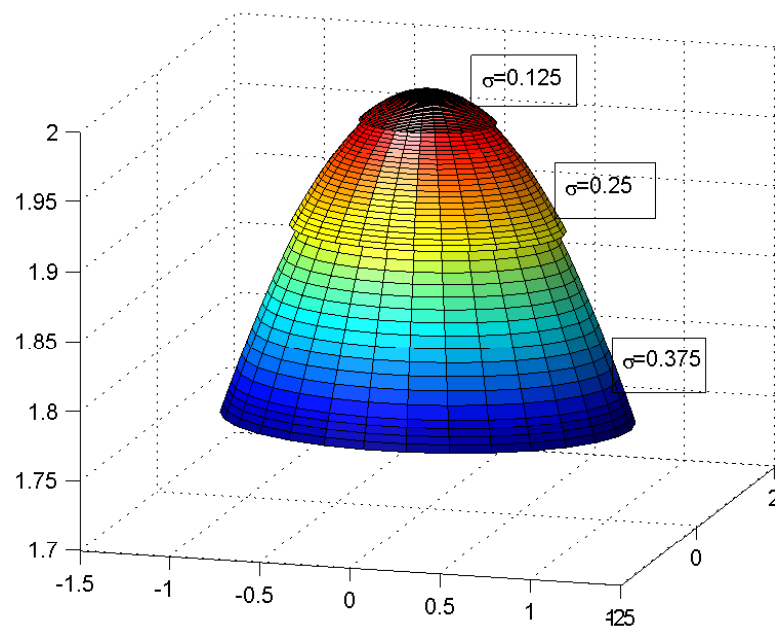Figure 3.2: Resulting surfaces for various parameter values σ.

Figure 3.3: Resulting surfaces with $z_0 = 2$ and parameters: $\sigma = 0.125$, $\sigma = 0.25$, $\sigma = 0.375$

In Figure 3.4, we generate a family of surfaces for a fixed parameter σ, namely $\sigma = 0.25$, but this time, using different initial conditions such as $z_0 = 1$, $z_0 = 1.2$ and $z_0 = 1.4$ in order to see the dependence of the solution on the initial value. In Figure 3.5, we combine all these surfeces in one to visualize all three at one place. We can see from the shape of these graphs that the larger the initial condition the steeper the surface of the reflector gets.
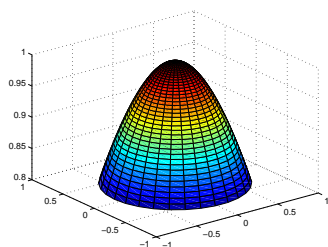
(a) Initial value: $z_0 = 1.0$ (b) Initial value: $z_0 = 1.2$
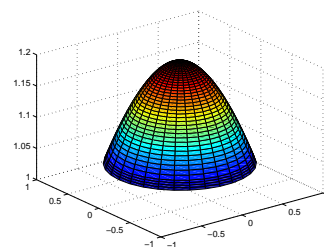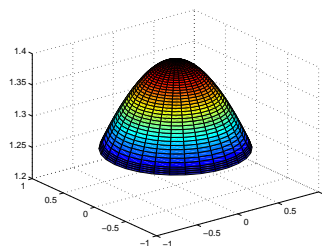
(c) Initial value: $z_0 = 1.4$

Figure 3.4: Resulting surfaces for various initial values z_0.
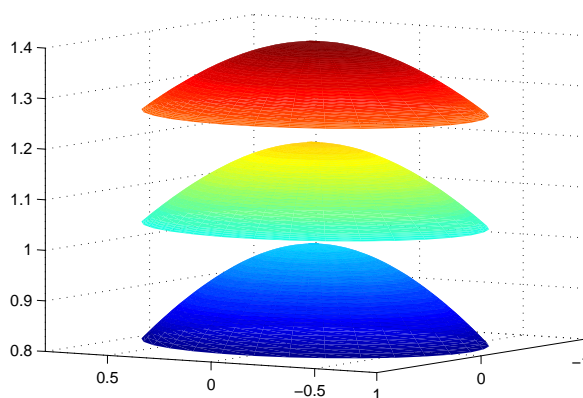
Figure 3.5: Surfaces with $\sigma = 0.25$ and different initial values: $z_0 = 1.0$, $z_0 = 1.2$ and $z_0 = 1.4$

In Figure 3.5 below, we have the deviations of the map γ for each of the parameters $\sigma = 0.125$, $\sigma = 0.25$ and $\sigma = 0.375$ with the same initial condition $z_0 = 2$. This set of graphs gives the amount of displacement of each ray of light over the surface $z = 0$.

Error analysis

When solving the ODE (3.27), the MATLAB code generates some data involving a vector $\vec{r}$ and the corresponding vectors containing values for z and z_r. Using them, we can test the consistency of the data.

Notice that we already have from (3.28)

$$\rho(r) = \frac{1 + (z_r)^2}{1 - (z_r)^2} z \tag{3.39}$$

which gives the distance between the point (r, z) where the ray is reflected and the image point $\gamma(r)$.

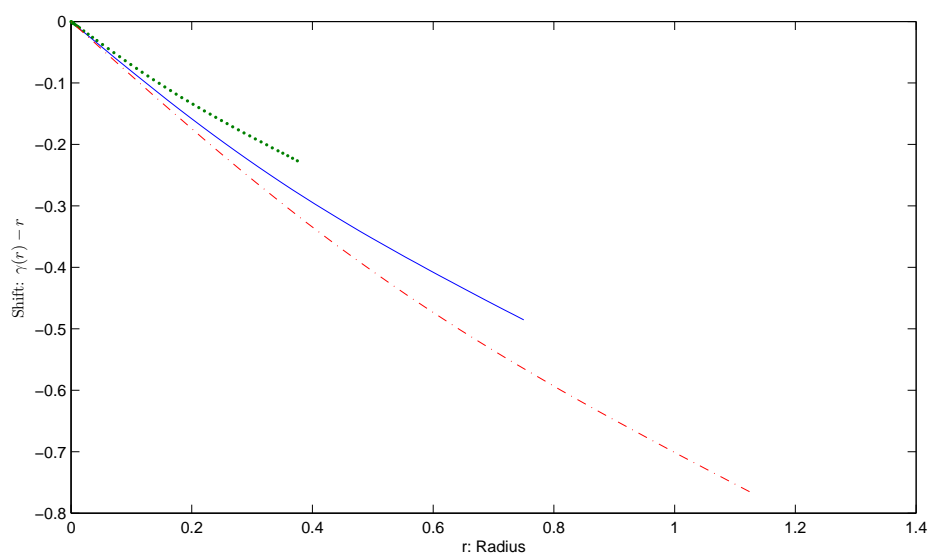On the other hand, using the Pythagorean rule, we also have the follow-

Figure 3.6: Deviations of the map γ for $\sigma = 0.125$, $\sigma = 0.25$, $\sigma = 0.375$ and initial value: $z_0 = 2$

ing:

$$\rho(r) = \sqrt{(r - \gamma(r))^2 + z^2}. \tag{3.40}$$

Then, requiring the equality of the equations (3.39) and (3.40), we can define an error function $\delta(r)$ as follows:

$$\delta(r) = \frac{1 + (z_r)^2}{1 - (z_r)^2} z - \sqrt{(r - \gamma(r))^2 + z^2}. \tag{3.41}$$

We would like the function γ to have values very close to 0. Figure 3.5 is a graph showing the r-$\delta(r)$ relation with the data generated by the ODE solver ode45.
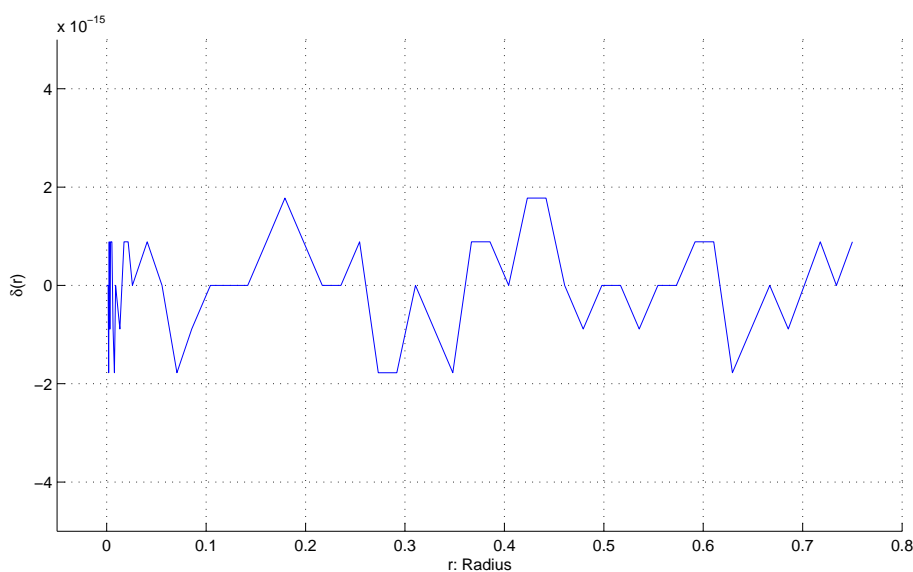
Figure 3.7: Error with parameter $\sigma = 2.5$ and initial value $z_0 = 2$

3.6 Conclusion

The problem of a collimated source was introduced and formulated in [11]. What we did was to redevelop the formula that is a nonlinear partial

differential equation of Monge-Ampère type. Then, we considered the rotationally symmetric case and deduced the formula applying to this particular case. Next, to illustrate the concept of rotational symmetry, we used our new formula and applied it to a specific example where a bell-shaped density was transformed into a uniform density. We generated surfaces giving the solution for several different cases, namely for the case when we have the same density parameter for different initial values of the problem and for the case when the same initial condition applies to different parameters.

We then observed that either changing the initial condition or changing the parameter clearly affects the shape of the resulting surface. We can easily conclude that increasing the parameter σ steepens the shape of the reflector, while increasing the initial condition z_0 flattens it.

Finally, we also produced a sketch of the error of the radial function at each $\gamma(r)$ depending on the distance r from the origin. We obtained a very satisfying result, as Figure 3.5 shows, our error function satisfies $|\delta(r)| \leq 2 \times 10^{-15}$.

Chapter 4

A Problem in Non-Imaging Optics

4.1 Introduction

Energy concentrators have played a significant role in energy production, especially since fossil fuels have become more challenging to acquire in most industrialized countries.

Concentrators have the goal of capturing radiant (solar) energy and transforming it into some other form of energy (like heat or electricity). Imaging the sun may be useful in solar astronomy or in the study of sun spots, but it has no obvious advantage in solar energy conversion systems. Thus, even if we take a more empirical optimization approach, it is plausible that relaxing the imaging requirement has the potential of improving concentration performance. Approaching the subject this way leads to incremental improvements over various classical imaging designs such as parabolic (or more generally convex) reflectors. In this chapter, our goal is to demonstrate methods of obtaining various models of concentrators. Note that these methods still resemble classical imaging approaches.

Consider an imaging problem, taking the simplest example of points on a line. An imaging system is required to map these points on another line, called the image, without scrambling the points −that is, to send the

rays issuing from every object point to their corresponding image points−. Each ray issuing from a point is represented by a straight line in the phase space, and the system is required to faithfully map line onto line. Now suppose we consider only the boundary of the beam of all rays. Then all we require that the boundary be transported from the source to the target. Due to the edge-ray principle, the interior rays will come along as seen in Figure 4.1. The interior rays cannot "leak out" because otherwise, by
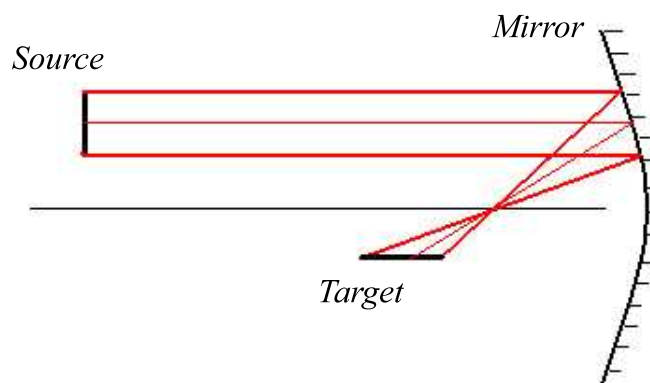
Figure 4.1: Light beam transmitted to target.

crossing the boundary, they would first become the boundary, and it is the boundary that is being transported. This looks pretty much like carrying a liquid inside a certain container. The fact that elements of the liquid inside the container mix or that the container itself is deformed has no importance as long as the content is transported. This is the key idea of nonimaging optics.

Nonimaging optics is mainly based on the fundamental studies of Welford and Winston ([27], [28]) and has recently been studied by the authors in [29] and many others.

In this chapter, we present several different types of concentrators. Different combinations of reflectors and refractors are considered. This leads to different levels of transmission, that is, percentages of light entering the concentrator that are absorbed by a target photocell.

4.2 Description of the Problem

We consider a system of two mirrors designed in such a way that the ray through any point $x \in \Omega$, where Ω is the initial domain on the plane $z = 0$, is carried after a couple of reflections to some point p in a target domain T_d located on the plane $z = d > 0$. We can think of Ω as the cross section of a collimated light beam B_0 in the direction parallel to the z-axis. The light beam B_0 reflects off the first and the second mirrors and takes its final form B_f, also parallel to the z-axis, and attains the target domain T_d.

Let us denote the intensity of the initial light beam as $I(x), x \in \Omega$ and the intensity of B_f as $L(p), p \in T_d$. Consequently, assuming preservation of total energy, we require the following balance condition:

$$\iint_\Omega I(x)dS_x = \iint_{T_d} L(p)dS_p. \tag{4.1}$$

Once this setup is constructed, it has been shown in [19] that the surface $z = z(x)$ of the first reflector is given by the solution of the following nonlinear PDE:

$$L(x + \beta \cdot \nabla z) \left| \det(Id + \beta \cdot \nabla^2 z) \right| = I(x), x \in \Omega \tag{4.2}$$

where β is a parameter.

The problem can now be described as following: Given the densities I on Ω and L on T_d, one is required to design a set of reflectors R_1 and R_2. Here, we want most of the total intensity hitting the first mirror R_1 to be
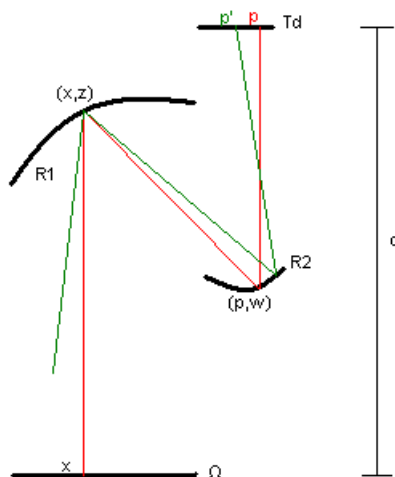
Figure 4.2: Two-mirror design (2-dimensional representation)

transmitted through the two-mirror reflector set and to reach the target domain T_d. We also want the collimated beam to have an incoming ray angle (angle of incidence) differing from the direction of the vertical z-axis as much as possible. A 2-dimensional representation of the setup is given in Figure 4.2. So, according to the figure, we want the green ray to make the greatest possible angle with the red ray for "almost" all points $(x, z) \in R_1$.

Here are a couple of definitions that will let us restate the problem in physical terms.

Definition 4.1. *The* transmission *(of light) is the percentage entering a certain optical system captured by the target set (receiver). It is sometimes called* efficiency.

Definition 4.2. *The* angle of acceptance, *usually denoted by* Δ, *is the maximum angle of incidence hitting the (first) surface of an optical system and satisfying a certain level of transmission.*

In general, the minimum transmission level required is considered to be 90%. The angle corresponding to this transmission level is called the real acceptance angle. Then, we can now restate the problem as designing an optical system that maximizes the acceptance angle for this specific transmission level.

The concentrator shown in Figure 4.2 is made up of a pair of reflecting surfaces. The rays initiated on the domain Ω are to be collected on the target (concentrator) set T_d located at a vertical distance of d units above the plane containing the light source Ω. The red rays are initially vertical and all those red rays are completely collected by the target. The solution to this problem is given in [19]. However, in the case of comatic wavefronts, that is, when the light rays do not have the initial vertical direction, the double-reflected rays will deviate from their initial image point in the target set T_d, and some of them (maybe most of them) will already be off-target. Our goal is to collect the majority of these rays for the largest possible angle of incidence. In this chapter, we discuss several different types of concentrators based on the idea described in the construction represented in Figure 4.2.

4.3 A Particular Design

We consider now a particular version of the problem above, namely, the rotationally symmetric case. In this case, the PDE (4.2) turns into a second order non-linear ODE. Without loss of generality, the density of the initial beam is uniformly assigned to be $I \equiv 1$, as we can assume that the sun's rays have a uniform distribution on any given surface. The solution to (4.2) is considered on a rectangular domain around the origin. The main difference in our setup is that we will use only the first mirror as the concentrator. In addition, the receiver cell will be placed at the very location of the second

surface as seen in Figure 4.3. The single-mirror setup provides us more control over the light that enters the system. In other words, it would be much more difficult for the light to hit the target cell after reflecting off two non-planar reflectors. The cell is modeled as a square of dimension 1cm×1cm while the mirror will be a surface lying above a domain of dimension 20cm×20cm in the plane $z = 0$. In the following example, we give the results for two different intensities pre-assigned for the target cell.
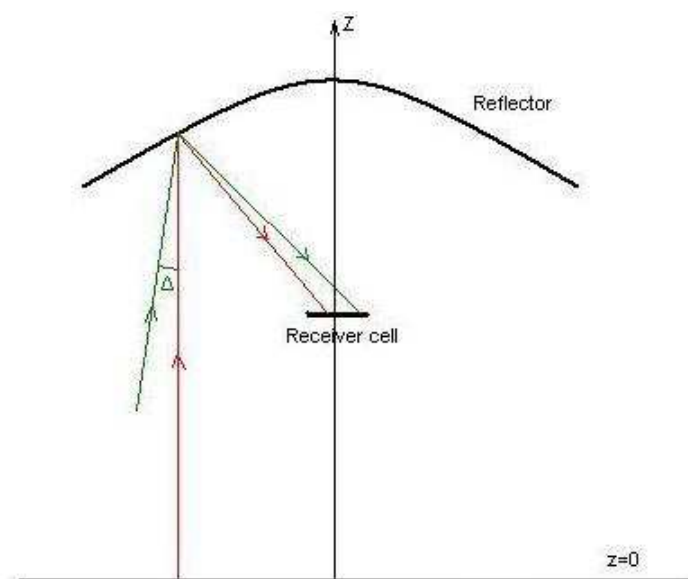
Figure 4.3: Single-mirror design

4.3.1 Example

In our first example, the reflecting surface is set to be lying above the domain $[-10, 10] \times [-10, 10]$ centered at the origin. We then present in Figure 4.4 some results for different pre-assignments of the parameter l in
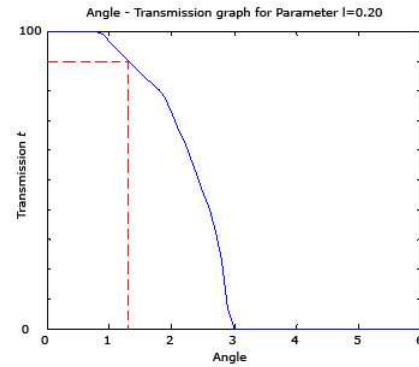
the uniform density function $L(p)$ given by:

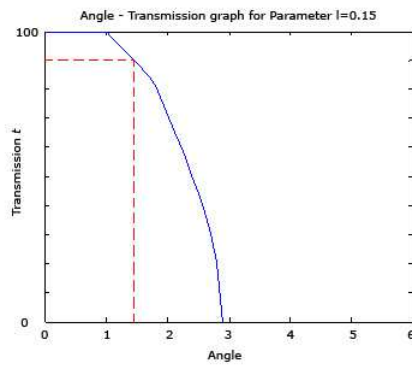$$L(p) = \begin{cases} c & \text{if } |p| < l \\ 0 & \text{otherwise} \end{cases} \tag{4.3}$$

where c is a constant to be determined and that satisfies the total energy balance condition. Next, we can work on the same construction, now using
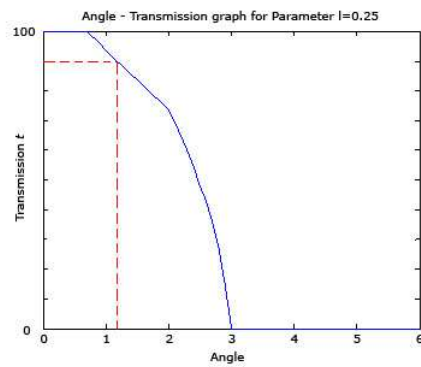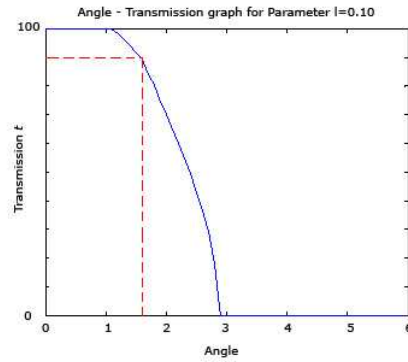

(a) Parameter $l = 0.25$ (b) Parameter $l = 0.20$

(c) Parameter $l = 0.15$ (d) Parameter $l = 0.10$

Figure 4.4: Results for an initially uniformly distributed intensity

a different density function L for the target set, defined as:

$$L(p) = \begin{cases} c \cdot e^{\frac{l^2}{l^2 - p^2}} & \text{if } |p| < l \\ 0 & \text{otherwise.} \end{cases} \tag{4.4}$$

This density provides a smoothly shaped distribution, as it is differentiable at all points on the target. We see in Figure 4.5 that the rays will fall off the target cell in a different manner compared to the case when the intensity is uniformly distributed. As a matter of fact, our main concern in nonimaging optics is to capture the maximum amount of light for the 90% transmission level. In this situation, it turns out that the density function given in 4.4 does not perform as well as the uniform density given in 4.3.

(a) Parameter $l = 0.25$

(b) Parameter $l = 0.20$

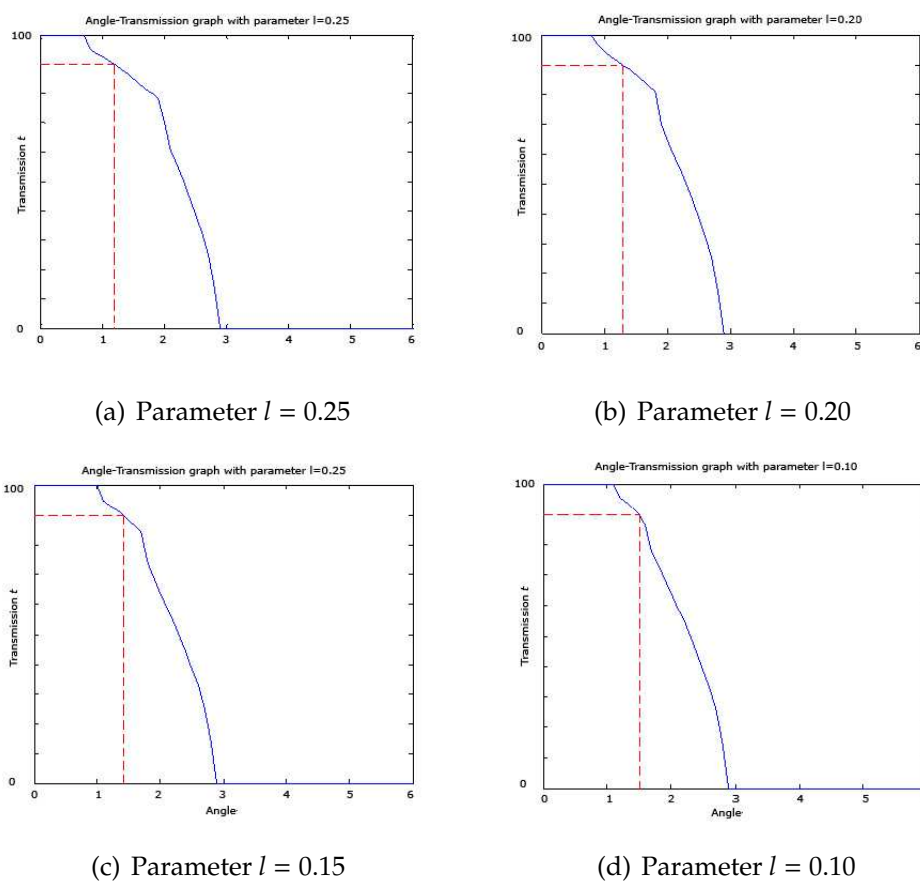(c) Parameter $l = 0.15$

(d) Parameter $l = 0.10$

Figure 4.5: Results for the intensity function (4.4)

4.4 A Mixed Design

The following construction, called the double medium-mirror design, is closely related to the previous one except for the mirror being located in a different medium. As seen in Figure 4.6, the rays first travel in Medium 1 with some refractive index n_1 and reach the edge of another medium (Medium 2) with refractive index n_2, where the incoming rays are refracted according to Snell's Law. In this design, we want Medium 2 to have a larger refractive index compared to that of Medium 1 ($n_1 < n_2$). For example, Medium 1 could be air with refractive index n_1 practically equal to 1, and Medium 2 could be the so-called soda-lime glass, whose refractive index is close to 1.5.
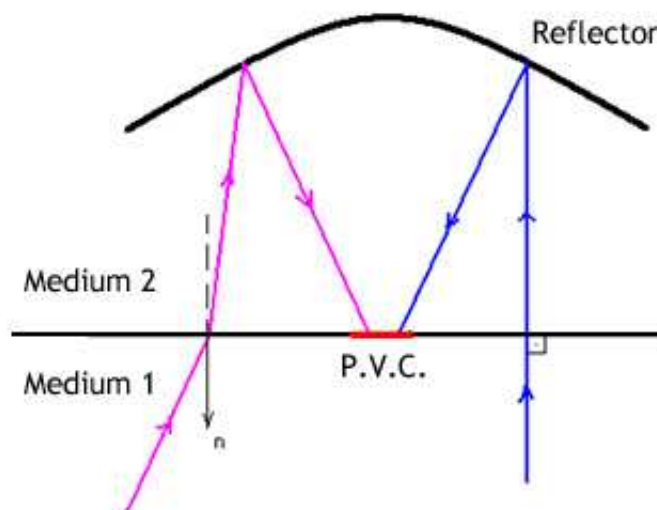

Figure 4.6: Double medium-mirror design

As we can see in Figure 4.6, the blue ray hits the refracting surface in the direction of the normal (i.e. perpendicularly), so no refraction occurs

in this case. If the purple ray has an angle of incidence $\theta_1 > 0$ with the normal to the surface of refraction, according to Snell's Law of Refraction

$$n_1 \cdot \sin \theta_1 = n_2 \cdot \sin \theta_2 \tag{4.5}$$

the angle of refraction θ_2 will be less than θ_1.

After the refraction, the light will travel in Medium 2, reflect back from the mirror and hopefully hit the Photovoltaic Cell (PVC), shown as a small red line segment in Figure 4.6. The advantage this construction provides is that the effect of the coma is reduced after the refraction because the refraction makes the rays bend towards the normal.

In this setup, the intensity on the target cell is the one given in 4.3 as:

$$L(p) = \begin{cases} c & \text{if } |p| < l \\ 0 & \text{otherwise} \end{cases} \tag{4.6}$$

where l is a parameter and c is the equilibrium constant satisfying the balancing condition (4.1). The parameter was chosen as $l = 1.2$ for this example.

The graph in Figure 4.7 shows the resulting transmission with a plain system (when there is no Medium II). We can see that the acceptance angle is 1.5 degrees.

Now, the following graph in Figure 4.8 gives the transmission of the system when Medium 1 is air ($n_1 = 1.000293$) and Medium 2 is soda-lime glass ($n_2 = 1.520$), which is the glass used for such objects as bottles and jars.

We can surely proceed further and make use of other materials with even higher refractive indices, for example, if we use Arsenic Trisulfide Glass, which has a refractive index higher than 2.3 [30], we obtain the angle-transmission graph presented in Figure 4.9.

The authors in [8] designed a concentrator using a method called the Simultaneous Multiple Surface (SMS), which involves both a refracting
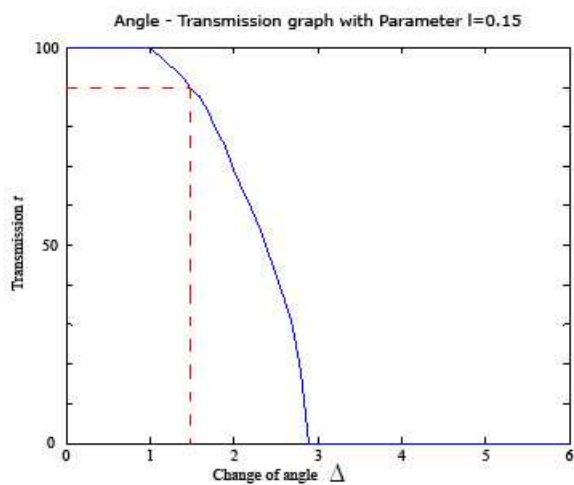
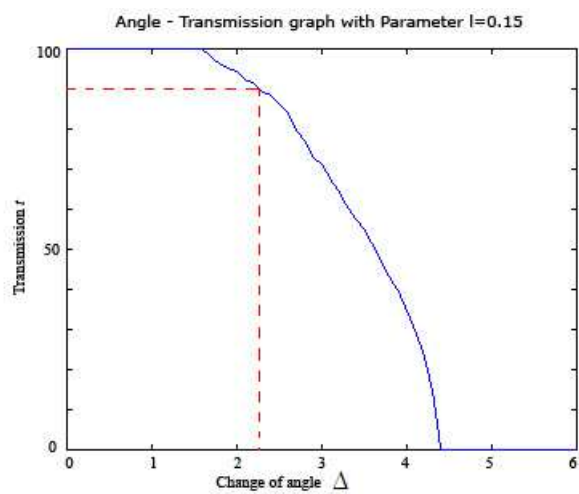Figure 4.7: Resulting transmission using a single-mirror design

Figure 4.8: Resulting transmission when the mirror lies in Soda-Lime Glass
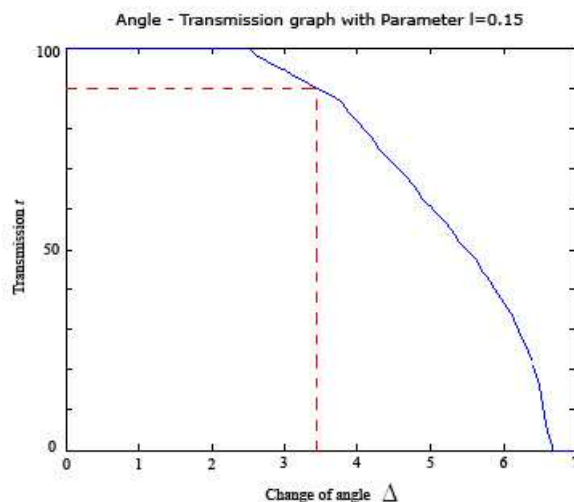
Figure 4.9: Resulting transmission when the mirror lies in Arsenic Trisulfide Glass

surface and a reflecting surface. In that system, the rays first hit a mirror and then a lens before reaching the photovoltaic cell. In our designs, the dimensions of the reflector measure 20cm × 20cm while the target cell is only 1cm × 1cm. This provides a concentration level of 400. According to previous results, also shown in [8], the acceptance angles of classical photovoltaic systems at this level of concentration do not exceed 1.5 degrees, which is approximately the level we actually obtained with the plain system shown in Figure 4.3.

As seen in the graphs in Figures 4.8 and 4.9, when the mirror and the concentrator are placed into different media, the acceptance angle that was initially as low as 1.5 degrees rose up to 2.2 degrees when that medium was the Soda-Lime Glass and to 3.2 degrees when we used Arsenic Trisulfide Glass. Theoretically, it is possible to use some material with an even higher refractive index and obtain better results.

4.5   A Refractive Surface

We now set up the problem above for the refractive surface case. That is, we reconsider the problem above and construct the surface of a lens instead of a mirror. So the design of the problem would be as described in Figure 4.10. In this construction, incoming rays first reach the lower side of the lens, which is planar. This side has no effect when incoming rays are perpendicular to the lower side of the lens, which is the case for the green ray in the figure. This green ray is refracted at the second side and is redirected toward the Photovoltaic Cell (PVC). The solution to the problem of determining the surfaces of a lens for pre-given incoming and outgoing collimated light intensities is given by Oliker [20]. We can make use of the solution given in [20] to construct the non-planar side of the lens. As a matter of fact, the solution to that problem is described as a pair of refracting surfaces that are called a two-lens by the author. This solution is given by a second order nonlinear partial differential equation of Monge-Ampère type.

   In our design, we consider the rotationally symmetric case. This lets us work on solving a second order non-linear ODE instead of a non-linear PDE of Monge-Ampère type. So we obtain a pair of surfaces of which we use only the first side (that is, the side of the lens that is reached first by the light rays). The PVC will then be placed right at the location of the second surface. Therefore, any collimated beam of light will be captured by the PVC, as the latter lies on the regular trajectory of the light rays. As seen in Figure 4.10, the green ray from a non-comatic radiation enters the lens and is refracted at the second surface in such a way that it is perfectly captured by the PVC. The blue ray, from the comatic beam of light, is refracted at both sides of the lens (as it does not have the direction of the normal to the first surface any more) and may or may not reach the target. To compare to
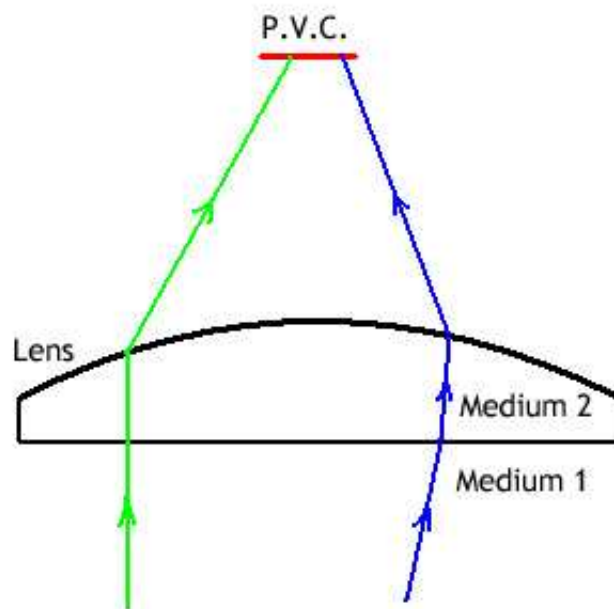
Figure 4.10: Single-lens design

previous designs, we set the dimensions as before to be 20cm×20cm for the lens and 1cm×1cm for the PVC. This also provides a concentration level of 400. The density used on the target set is initially set as uniform and the initial parameter used on the target set is $l = 0.15$.
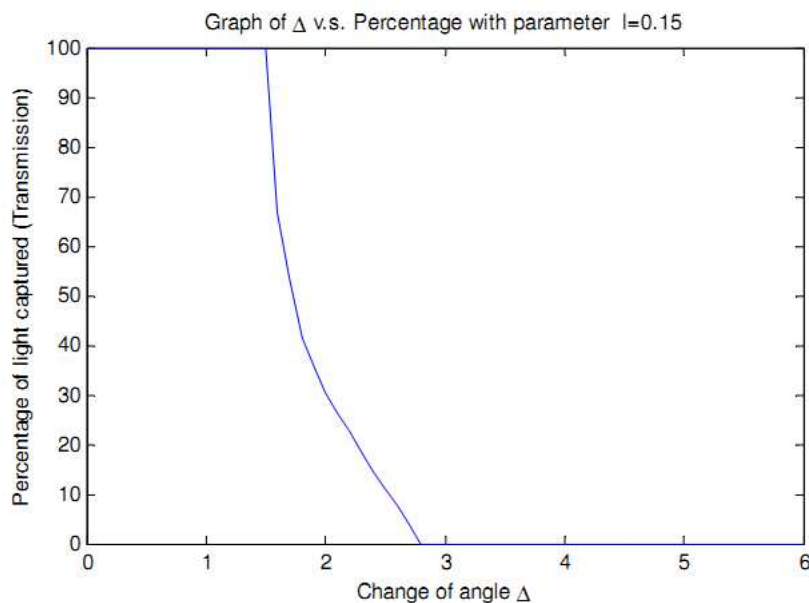

Figure 4.11: Angle transmission graph when n=1.5

For our first example, whose results are given in Figure 4.11, we have the angle-transmission graph for the case when the material used is the usual Soda-Lime Glass with refractive index set to $n = 1.5$.

Our next example gives the result of the same design only when we make a change in the material used for the construction of the lens and use Potassium Niobate ($KNbO_3$) instead of the regular glass. The corresponding results are given in Figure 4.12.

To emphasize the dependency on the refractive index of the material, we also verified the setup with material of even larger index of refraction. The

use of silicon whose index of refraction is $n = 3.96$ generates the results in Figure 4.13.
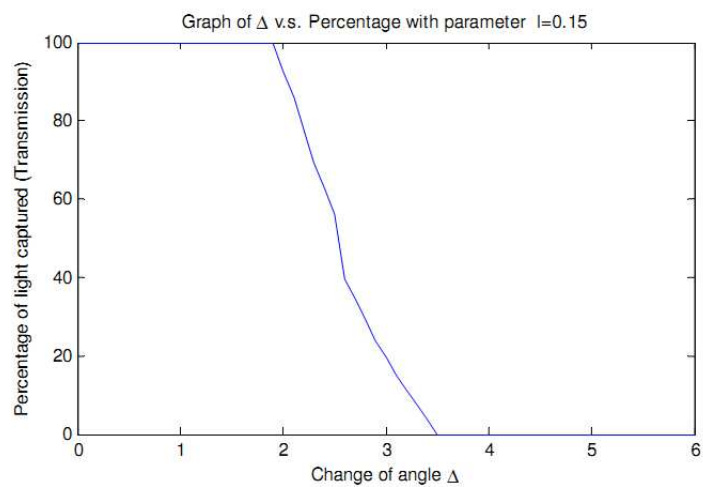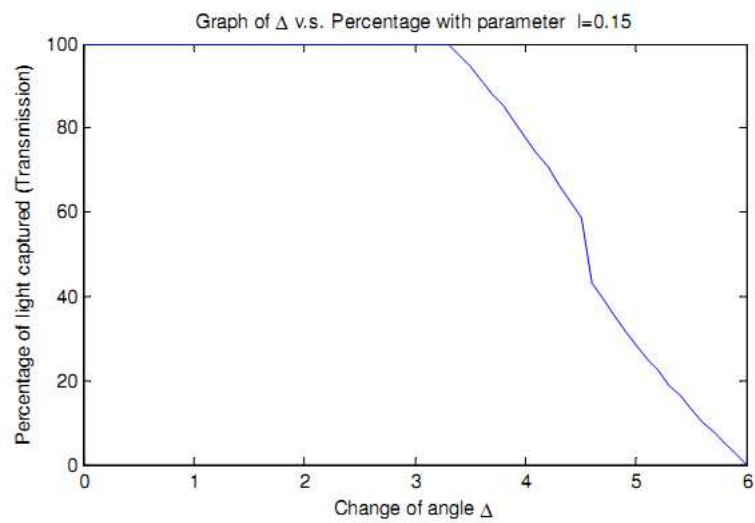

Figure 4.12: Angle transmission graph when n=2.28

Figure 4.13: Angle transmission graph when n=3.96

Bibliography

[1] L.A. Caffarelli and V.I. Oliker, Weak solutions of one inverse problem, J. Math. Sc., **154** (1), pp. 39-49 (2008).

[2] F. R. Fournier, W. J. Cassarly and J. P. Rolland, Fast freeform reflector generation using source-target maps, Optics Express, **18** (5), pp. 5295-5304 (2010).

[3] F. R. Fournier, W. J. Cassarly and J. P. Rolland, Freeform Reflector Design Using Integrable Maps, in *Proceedings of the International Optical Design Conference*, Jackson Hole Wyoming, 2010.

[4] F. R. Fournier and W. J. Cassarly and J. P. Rolland, Designing freeform reflectors for extended sources, in *SPIE Nonimaging Optics: Efficient Design for Illumination and Solar Concentration VI*, SPIE Vol. 7423:203-214, San Diego, 2009.

[5] B.R. Frieden, Lossless conversion of a plane laser wave to a plane wave of uniform radiation, Appl. Opt., **4**, pp. 1400-1403 (1965).

[6] T. Glimm, A rigorous analysis using optimal transport theory for a two-reflector design problem with a point source, Inverse Problems, **26** (4), pp. 1-16 (2010).

[7] C.E. Gutiérrez and Q. Huang, The refractor problem in reshaping light beams, Arch. Rational Mech. Anal., **193**, pp. 423-443 (2009).

[8] M. Hernández, P. Benítez, J. C. Miñano, A. Cvetkovic, R. Mohedano, O. Dross, R. Jones, D. Whelan, G. S. Kinsey, and R. Alvarez, The XR nonimaging photovoltaic concentrator, Nonimaging Optics and Efficient Illumination Systems IV. Proceedings SPIE 2007, Vol. 6670.

[9] T. Glimm and V. Oliker, Optical design of two-reflector systems, the Monge-Kantorovich mass transfer problem and Fermat's principle, Indiana U. Math. J., **53** (5), pp. 1255-1278 (2004).

[10] A. Karakhanyan, On the regularity of weak solutions to refractor problem, Arm. J. Math., **2** (1), pp. 28-37 (2009).

[11] S.A. Kochengin, Reflector construction problems, Ph.D. dissertation, Emory University (1999).

[12] S.A. Kochengin and V.I. Oliker, Determination of reflector surfaces from near field scattering data, Inv. Problems, **13**, pp. 363-373 (1997).

[13] J.L. Kreuzer, Coherent light optical system yielding an output beam of desired intensity distribution at a desired equiphase surface, U.S. Patent No. 3,476,463 (1969).

[14] S. Magarill, Anamorphic illuminator, in *Proceedings of SPIE. Nonimaging Optics: Efficient Design for Illumination and Solar Concentration VII (Conference 7785), edited by R. Winston, J.M. Gordon*, 7785-18,2010.

[15] D. Michaelis, S. Kudaev, R. Steinkopf, A. Gebhardt, P. Schreiber and A. Bräuer, Incoherent beam shaping with freeform mirror, in *Proceedings of SPIE. Nonimaging Optics and Efficient Illumination Systems V, edited by R. Winston, R. J. Koshel*, 7059(705905): 1-05, 2008.

[16] D. Mountford, Refraction properties of conics, Math. Gaz., **68** (444), pp. 134-137 (1984).

[17] R. S. Mulder, Shape and illumination as a function of path length, in *SPIE Nonimaging Optics and Efficient Illumination Systems IV, edited by R. Winston, R. J. Koshel*,66700P, 13 pages, 2007.

[18] J.A. Nelder and R. Mead, A simplex method for function minimization, Comp. J., **7**, pp. 308-313 (1965).

[19] V.I. Oliker, Optical design of freeform two-mirror beam-shaping systems, J.Opt. Soc. Am. A, **24** (12), pp. 3741-3752 (2007).

[20] V.I. Oliker, On design of free-form refractive beam shapers, sensitivity to figure error, and convexity of lenses, J. Opt. Soc. Am. A, **25** (12), pp. 3067-3076 (2008).

[21] V.I. Oliker, Designing freeform lenses for intensity and phase control of coherent light with help from geometry and mass transport, Arch. Rational Mech. Anal., **201** (3), pp. 1013-1045 (2011).

[22] M.J.D. Powell, An efficient method for finding the minimum of a function of several variables without calculating derivatives, Comp. J., **7**, pp. 155-162 (1964).

[23] H. H. Rosenbrock, An automatic method for finding the greatest or least value of a function, Comp. J., **3** (3), pp. 175-184 (1960).

[24] J. Rubinstein and G. Wolansky, A weighted least action principle for dispersive waves, Ann. Phys., **317**, pp. 271-284 (2005).

[25] J. Rubinstein and G. Wolansky, Intensity control with a free-form lens, J. Opt. Soc. Am. A, **24** (2), pp. 463-469 (2007).

[26] X. Wang, On the design of a reflector antenna, Inverse Problems, **12**, pp. 351-375 (1996).

[27] W.T. Welford and R. Winston, *The optics of nonimaging concentrators: light and solar energy*, Academic Press, New York, 1978.

[28] W.T. Welford and R. Winston, *High collection nonimaging optics*, Academic Press, New York, 1989.

[29] R. Winston, J.C. Miñano, and Benítez, *Nonimaging optics*, Elsevier Academic Press, Oxford, UK, 2005.

[30] P.A. Young, Reflectivity of vitreous arsenic trisulfide, Appl. Opt., **10**, pp. 222-223 (1971).